SANDIA REPORT

SAND2004-2143
Unlimited Release
Printed May 2004

Laminated Composites Modeling in ADAGIO/PRESTO

Daniel C. Hammerand

Prepared by Sandia National Laboratories
Albuquerque, New Mexico 87185 and Livermore, California 94550

Sandia is a multiprogram laboratory operated by Sandia Corporation,
a Lockheed Martin Company, for the United States Department of Energy's
National Nuclear Security Administration under Contract DE-AC04-94AL85000.

Approved for public release; further dissemination unlimited.

Sandia National Laboratories

Issued by Sandia National Laboratories, operated for the United States Department of Energy by Sandia Corporation.

Printed in the United States of America. This report has been reproduced directly from the best available copy.

Available to DOE and DOE contractors from
U.S. Department of Energy
Office of Scientific and Technical Information
P.O. Box 62
Oak Ridge, TN 37831

Telephone: (865)576-8401
Facsimile: (865)576-5728
E-Mail: reports@adonis.osti.gov
Online ordering: http://www.osti.gov/bridge

Available to the public from
U.S. Department of Commerce
National Technical Information Service
5285 Port Royal Rd
Springfield, VA 22161

Telephone: (800)553-6847
Facsimile: (703)605-6900
E-Mail: orders@ntis.fedworld.gov
Online order: http://www.ntis.gov/help/ordermethods.asp?loc=7-4-0#online

SAND2004-XXXX
Printed XXXX 2004

Laminated Composites Modeling in ADAGIO/PRESTO

Daniel C. Hammerand
Material Mechanics
Sandia National Laboratories
P.O. Box 5800
Albuquerque, NM 87185-0893

Abstract

A linear elastic constitutive equation for modeling fiber-reinforced laminated composites via shell elements is specified. The effects of transverse shear are included using first-order shear deformation theory. The proposed model is written in a rate form for numerical evaluation in the Sandia quasi-statics code ADAGIO and explicit dynamics code PRESTO. The equation for the critical time step needed for explicit dynamics is listed assuming that a flat bilinear Mindlin shell element is used in the finite element representation. Details of the finite element implementation and usage are given. Finally, some of the verification examples that have been included in the ADAGIO regression test suite are presented.

Acknowledgments

The work performed by Vicki Porter in creating the necessary interface coding between the shell element and the developed material model is very much appreciated, as is the coding performed by Tim Walsh to partially create the user-defined coordinate systems for material initialization. The author also gratefully acknowledges the many helpful comments and suggestions provided by the reviewers Bob Chambers and Bill Scherzinger.

Contents

List of Figures

List of Tables

1 Constitutive Model

The small to moderate material distortion response of laminated plates and shells composed of fiber-reinforced polymer matrix laminae is consistent with generalized plane stress assumptions. However, even under generalized plane stress assumptions, there are two general approaches to modeling the constitutive response of the lay-up. The first approach is to handle the material response of each lamina separately. The second approach is to determine an equivalent laminate constitutive model corresponding to pre-integrating the material response through the thickness under an assumed variation of strain through the thickness. The first approach requires the analyst to specify a stacking sequence, whereas the second approach does not. However, the orientation of the laminate as a whole still must be specified for the second approach. This report describes the `elastic_laminate` model which follows the second approach.

1.1 Constitutive Equations for the k^{th} Layer

Before reducing to plane stress conditions, the 3-D orthotropic linear elastic material law for the k^{th} layer is written in rate form as follows:

$$\left\{\begin{array}{c} \dot{\epsilon}_{11}^k \\ \dot{\epsilon}_{22}^k \\ \dot{\epsilon}_{33}^k \\ 2\dot{\epsilon}_{23}^k \\ 2\dot{\epsilon}_{31}^k \\ 2\dot{\epsilon}_{12}^k \end{array}\right\} = \begin{bmatrix} \frac{1}{E_1^k} & -\frac{\nu_{21}^k}{E_2^k} & -\frac{\nu_{31}^k}{E_3^k} & 0 & 0 & 0 \\ -\frac{\nu_{12}^k}{E_1^k} & \frac{1}{E_2^k} & -\frac{\nu_{32}^k}{E_3^k} & 0 & 0 & 0 \\ -\frac{\nu_{13}^k}{E_1^k} & -\frac{\nu_{23}^k}{E_2^k} & \frac{1}{E_3^k} & 0 & 0 & 0 \\ 0 & 0 & 0 & \frac{1}{G_{23}^k} & 0 & 0 \\ 0 & 0 & 0 & 0 & \frac{1}{G_{31}^k} & 0 \\ 0 & 0 & 0 & 0 & 0 & \frac{1}{G_{12}^k} \end{bmatrix} \left\{\begin{array}{c} \dot{\sigma}_{11}^k \\ \dot{\sigma}_{22}^k \\ \dot{\sigma}_{33}^k \\ \dot{\sigma}_{23}^k \\ \dot{\sigma}_{31}^k \\ \dot{\sigma}_{12}^k \end{array}\right\} + \dot{T}\left\{\begin{array}{c} \alpha_1^k \\ \alpha_2^k \\ \alpha_3^k \\ 0 \\ 0 \\ 0 \end{array}\right\} \tag{1.1}$$

where 1 and 2 denote the inplane principal material directions, 3 denotes the thickness direction, $\dot{\sigma}_{ij}$ is the ij component of mechanical stress rate, $\dot{\epsilon}_{ij}$ is the ij component of the total strain rate, and E_i^k, ν_{ij}^k, G_{ij}^k, and α_i^k are the engineering properties. Here it is observed that the total strain rate has been decomposed into mechanical and thermal parts. Because an elastic potential or strain energy density function exists for such an orthotropic model, the constitutive matrix is symmetric and the following relations hold:

$$\frac{\nu_{ij}^k}{E_i^k} = \frac{\nu_{ji}^k}{E_j^k} \quad \text{for } i, j = 1, 2, 3 \tag{1.2}$$

Applying generalized plane stress conditions ($\sigma_{33} = 0$) to Eq. (1.1) yields the following thickness strain rate:

$$\dot{\epsilon}_{33}^k = -\frac{\nu_{13}^k}{E_1^k}\dot{\sigma}_{11}^k - \frac{\nu_{23}^k}{E_2^k}\dot{\sigma}_{22}^k + \alpha_3^k \dot{T} \tag{1.3}$$

However, the effects of thickness strain will be assumed to be negligible in integrating the material response through the thickness.

Eliminating $\dot{\sigma}_{33}^k$ and $\dot{\epsilon}_{33}^k$ from Eq. (1.1) and inverting gives

$$\left\{ \begin{array}{c} \dot{\sigma}_{11}^k \\ \dot{\sigma}_{22}^k \\ \dot{\sigma}_{23}^k \\ \dot{\sigma}_{31}^k \\ \dot{\sigma}_{12}^k \end{array} \right\} = \left[\begin{array}{ccccc} Q_{11}^k & Q_{12}^k & 0 & 0 & 0 \\ Q_{12}^k & Q_{22}^k & 0 & 0 & 0 \\ 0 & 0 & Q_{44}^k & 0 & 0 \\ 0 & 0 & 0 & Q_{55}^k & 0 \\ 0 & 0 & 0 & 0 & Q_{66}^k \end{array} \right] \left\{ \left\{ \begin{array}{c} \dot{\epsilon}_{11}^k \\ \dot{\epsilon}_{22}^k \\ 2\dot{\epsilon}_{23}^k \\ 2\dot{\epsilon}_{31}^k \\ 2\dot{\epsilon}_{12}^k \end{array} \right\} - \dot{T} \left\{ \begin{array}{c} \alpha_1^k \\ \alpha_2^k \\ 0 \\ 0 \\ 0 \end{array} \right\} \right\} \tag{1.4}$$

Note that the mechanical stress rate depends linearly on the mechanical strain rate which is determined as the difference between the total/kinematic and thermal strain rates.

The reduced stiffnesses Q_{ij}^k are given in terms of the engineering properties as follows:

$$Q_{11}^k = \frac{E_1^k}{1 - \nu_{12}^k \nu_{21}^k} \tag{1.5}$$

$$Q_{22}^k = \frac{E_2^k}{1 - \nu_{12}^k \nu_{21}^k} \tag{1.6}$$

$$Q_{12}^k = \frac{\nu_{12}^k E_2^k}{1 - \nu_{12}^k \nu_{21}^k} = \frac{\nu_{21}^k E_1^k}{1 - \nu_{12}^k \nu_{21}^k} \tag{1.7}$$

$$Q_{44}^k = G_{23}^k \tag{1.8}$$

$$Q_{55}^k = G_{31}^k \tag{1.9}$$

$$Q_{66}^k = G_{12}^k \tag{1.10}$$

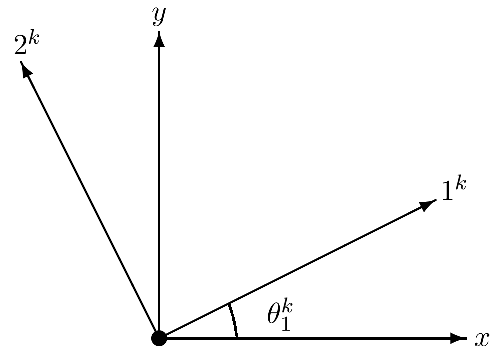

Figure 1.1: Material (1^k-2^k-3^k) and user-defined (x-y-z) coordinate systems. The material and user-defined coordinate systems share a common axis which is perpendicular to the shell surface (3^k & z) and differ by a rotation of θ_1^k about this axis.

Using standard tensor transformation techniques, the constitutive equation for each lamina given by Eq. (1.4) can be rewritten using a single user-defined x-y-z coordinate system. This x-y-z system is related to the 1^k-2^k-3^k system by a single rotation of magnitude θ_1^k about the 3^k axis as shown in Fig. 1.1. Both of these coordinate systems share an axis (3^k and z) which is perpendicular to the shell surface. Although not shown, a X_g-Y_g-Z_g global coordinate system exists. Note that since the user-defined system has the x-y plane tangent to the shell surface, the user-defined system is usually not aligned with the global coordinate system. Also note that it is likely that the material directions for each layer differ from each other.

Standard tensor transformations are used to transform the constitutive equation for the k^{th} layer to the x-y-z user-defined coordinate system. The following decoupled sets of equations result:

$$\left\{ \begin{array}{c} \dot{\sigma}_{xx}^k \\ \dot{\sigma}_{yy}^k \\ \dot{\sigma}_{xy}^k \end{array} \right\} = \left[\begin{array}{ccc} \bar{Q}_{11}^k & \bar{Q}_{12}^k & \bar{Q}_{16}^k \\ \bar{Q}_{12}^k & \bar{Q}_{22}^k & \bar{Q}_{26}^k \\ \bar{Q}_{16}^k & \bar{Q}_{26}^k & \bar{Q}_{66}^k \end{array} \right] \left\{ \left\{ \begin{array}{c} \dot{\epsilon}_{xx}^k \\ \dot{\epsilon}_{yy}^k \\ 2\dot{\epsilon}_{xy}^k \end{array} \right\} - \dot{T} \left\{ \begin{array}{c} \alpha_{xx}^k \\ \alpha_{yy}^k \\ 2\alpha_{xy}^k \end{array} \right\} \right\} \tag{1.11}$$

and

$$\left\{ \begin{array}{c} \dot{\sigma}_{yz}^k \\ \dot{\sigma}_{zx}^k \end{array} \right\} = \left[\begin{array}{cc} \bar{Q}_{44}^k & \bar{Q}_{45}^k \\ \bar{Q}_{45}^k & \bar{Q}_{55}^k \end{array} \right] \left\{ \begin{array}{c} 2\dot{\epsilon}_{yz}^k \\ 2\dot{\epsilon}_{zx}^k \end{array} \right\} \tag{1.12}$$

The transformed reduced stiffnesses ($\bar{Q}^k_{ij}$'s) are given by

$$\begin{bmatrix} \bar{Q}^k_{11} & \bar{Q}^k_{12} & \bar{Q}^k_{16} \\ \bar{Q}^k_{12} & \bar{Q}^k_{22} & \bar{Q}^k_{26} \\ \bar{Q}^k_{16} & \bar{Q}^k_{26} & \bar{Q}^k_{66} \end{bmatrix} = \left[P_1(\theta^k_1)\right]^{-1} \begin{bmatrix} Q^k_{11} & Q^k_{12} & 0 \\ Q^k_{12} & Q^k_{22} & 0 \\ 0 & 0 & Q^k_{66} \end{bmatrix} \left[P_1(\theta^k_1)\right]^{-T} \tag{1.13}$$

and

$$\begin{bmatrix} \bar{Q}^k_{44} & \bar{Q}^k_{45} \\ \bar{Q}^k_{45} & \bar{Q}^k_{55} \end{bmatrix} = \left[P_2(\theta^k_1)\right]^{-1} \begin{bmatrix} Q^k_{44} & 0 \\ 0 & Q^k_{55} \end{bmatrix} \left[P_2(\theta^k_1)\right]^{-T} \tag{1.14}$$

where

$$[P_1(\theta)] = \begin{bmatrix} \cos^2\theta & \sin^2\theta & 2\sin\theta\cos\theta \\ \sin^2\theta & \cos^2\theta & -2\sin\theta\cos\theta \\ -\sin\theta\cos\theta & \sin\theta\cos\theta & \cos^2\theta - \sin^2\theta \end{bmatrix} \tag{1.15}$$

and

$$[P_2(\theta)] = \begin{bmatrix} \cos\theta & -\sin\theta \\ \sin\theta & \cos\theta \end{bmatrix} \tag{1.16}$$

The transformed coefficients of thermal expansion (CTE's) are determined from those in the principal material directions as follows:

$$\begin{Bmatrix} \alpha^k_{xx} \\ \alpha^k_{yy} \\ \alpha^k_{xy} \end{Bmatrix} = \left[P_1(\theta^k)\right]^{-1} \begin{Bmatrix} \alpha^k_1 \\ \alpha^k_2 \\ 0 \end{Bmatrix} \tag{1.17}$$

Equation (1.17) shows that non-zero α^k_{xy} can result for a chosen x-y-z coordinate system, even though, physically, thermal variations only lead to extensional strains when observed in a coordinate system aligned with the principal material directions.

Equations (1.11) and (1.12) are written in condensed notation as follows:

$$\left\{\dot{\sigma}^k\right\} = \left[\bar{Q}^k\right] \left\{\left\{\dot{\epsilon}^k\right\} - \dot{T}\left\{\alpha^k\right\}\right\} \tag{1.18}$$

and

$$\left\{\dot{\sigma}^k_{ts}\right\} = \left[\bar{Q}^k_{ts}\right] \left\{\dot{\epsilon}^k_{ts}\right\} \tag{1.19}$$

where the transverse shear quantities are differentiated from the inplane quantities by the ts subscript.

1.2 Laminate Response In User-defined Coordinate System

First-order shear deformation theory is used to express the thickness variation of the strain rates in terms of midplane quantities. The user-defined coordinate system is now restricted to the case where the midplane location is described by $z = 0$. The total inplane kinematic strain rates vary linearly through the thickness as follows:

$$\left\{ \begin{array}{c} \dot{\epsilon}_{xx} \\ \dot{\epsilon}_{yy} \\ 2\dot{\epsilon}_{xy} \end{array} \right\} = \left\{ \begin{array}{c} \dot{e}_{xx} \\ \dot{e}_{yy} \\ 2\dot{e}_{xy} \end{array} \right\} + z \left\{ \begin{array}{c} \dot{\kappa}_{xx} \\ \dot{\kappa}_{yy} \\ 2\dot{\kappa}_{xy} \end{array} \right\} \tag{1.20}$$

where e_{ij} and κ_{ij}, respectively, are midplane strains and bending curvatures. The transverse shear strains are assumed to be constant throughout the thickness and are expressed as

$$\left\{ \begin{array}{c} 2\dot{\epsilon}_{yz} \\ 2\dot{\epsilon}_{zx} \end{array} \right\} = \left\{ \begin{array}{c} 2\dot{e}_{yz} \\ 2\dot{e}_{zx} \end{array} \right\} \tag{1.21}$$

Equations (1.20) and (1.21), respectively, are written in compacted notation as

$$\{\dot{\epsilon}\} = \{e\} + z\,\{\kappa\} \tag{1.22}$$

and

$$\{\dot{\epsilon}_{ts}\} = \{\dot{e}_{ts}\} \tag{1.23}$$

Recall that when thermal variations are applied, only the mechanical portion of the total strain rate will result in mechanical stress.

The laminate material behavior is described in terms of force resultants N_{ij} and force-couple resultants M_{ij} which are defined as follows:

$$\left\{ \begin{array}{c} N_{xx} \\ N_{yy} \\ N_{xy} \end{array} \right\} = \int_{-h/2}^{h/2} \left\{ \begin{array}{c} \sigma_{xx} \\ \sigma_{yy} \\ \sigma_{xy} \end{array} \right\} dz \quad \text{or} \quad \{N\} = \int_{-h/2}^{h/2} \{\sigma\}\, dz \tag{1.24}$$

$$\left\{ \begin{array}{c} N_{yz} \\ N_{zx} \end{array} \right\} = \int_{-h/2}^{h/2} \left\{ \begin{array}{c} \sigma_{yz} \\ \sigma_{zx} \end{array} \right\} dz \quad \text{or} \quad \{N_{ts}\} = \int_{-h/2}^{h/2} \{\sigma_{ts}\}\, dz \tag{1.25}$$

$$\left\{ \begin{array}{c} M_{xx} \\ M_{yy} \\ M_{xy} \end{array} \right\} = \int_{-h/2}^{h/2} z \left\{ \begin{array}{c} \sigma_{xx} \\ \sigma_{yy} \\ \sigma_{xy} \end{array} \right\} dz \quad \text{or} \quad \{M\} = \int_{-h/2}^{h/2} z\,\{\sigma\}\, dz \tag{1.26}$$

where h is the laminate thickness. Note that integrating $z\{\sigma_{ts}\}$ through the thickness produces no net moments, because $\{\dot{\epsilon}_{ts}\}$ is uniform through the thickness.

Using the kinematic assumptions expressed in Eqs. (1.20) and (1.21) and incorporating thermal strains, the following laminate material model results:

$$\left\{\begin{array}{c}\dot{N}_{xx}\\ \dot{N}_{yy}\\ \dot{N}_{xy}\\ \dot{M}_{xx}\\ \dot{M}_{yy}\\ \dot{M}_{xy}\end{array}\right\}=\left[\begin{array}{ccc|ccc}A_{11}&A_{12}&A_{16}&B_{11}&B_{12}&B_{16}\\ A_{12}&A_{22}&A_{26}&B_{12}&B_{22}&B_{26}\\ A_{16}&A_{26}&A_{66}&B_{16}&B_{26}&B_{66}\\ \hline B_{11}&B_{12}&B_{16}&D_{11}&D_{12}&D_{16}\\ B_{12}&B_{22}&B_{26}&D_{12}&D_{22}&D_{26}\\ B_{16}&B_{26}&B_{66}&D_{16}&D_{26}&D_{66}\end{array}\right]\left\{\begin{array}{c}\dot{e}_{xx}\\ \dot{e}_{yy}\\ 2\dot{e}_{xy}\\ \dot{\kappa}_{xx}\\ \dot{\kappa}_{yy}\\ 2\dot{\kappa}_{xy}\end{array}\right\}-\dot{T}\left\{\begin{array}{c}N^{th}_{xx}\\ N^{th}_{yy}\\ N^{th}_{xy}\\ M^{th}_{xx}\\ M^{th}_{yy}\\ M^{th}_{xy}\end{array}\right\} \tag{1.27}$$

and

$$\left\{\begin{array}{c}\dot{N}_{yz}\\ \dot{N}_{zx}\end{array}\right\}=\left[\begin{array}{cc}A_{44}&A_{45}\\ A_{45}&A_{55}\end{array}\right]\left\{\begin{array}{c}2\dot{e}_{yz}\\ 2\dot{e}_{zx}\end{array}\right\} \tag{1.28}$$

where

$$A_{ij} = \int_{-h/2}^{h/2} \bar{Q}^k_{ij}\, dz \tag{1.29}$$

$$B_{ij} = \int_{-h/2}^{h/2} z\bar{Q}^k_{ij}\, dz \tag{1.30}$$

$$D_{ij} = \int_{-h/2}^{h/2} z^2\bar{Q}^k_{ij}\, dz \tag{1.31}$$

and the constant portion of the thermal force and force-couple resultants are given by

$$\left\{\begin{array}{c}N^{th}_{xx}\\ N^{th}_{yy}\\ N^{th}_{xy}\end{array}\right\}=\int_{-h/2}^{h/2}\left[\bar{Q}^k\right]\left\{\begin{array}{c}\alpha^k_{xx}\\ \alpha^k_{yy}\\ 2\alpha^k_{xy}\end{array}\right\}dz \tag{1.32}$$

and

$$\left\{\begin{array}{c}M^{th}_{xx}\\ M^{th}_{yy}\\ M^{th}_{xy}\end{array}\right\}=\int_{-h/2}^{h/2}z\left[\bar{Q}^k\right]\left\{\begin{array}{c}\alpha^k_{xx}\\ \alpha^k_{yy}\\ 2\alpha^k_{xy}\end{array}\right\}dz \tag{1.33}$$

In compacted notation, Eqs. (1.27) and (1.28), respectively, are given by

$$\left\{\begin{array}{c}\left\{\dot{N}\right\}\\ \left\{\dot{M}\right\}\end{array}\right\}=\left[\begin{array}{cc}[A]&[B]\\ [B]&[D]\end{array}\right]\left\{\begin{array}{c}\{\dot{e}\}\\ \{\dot{\kappa}\}\end{array}\right\}-\dot{T}\left\{\begin{array}{c}\left\{N^{th}\right\}\\ \left\{M^{th}\right\}\end{array}\right\} \tag{1.34}$$

and

$$\left\{\dot{N}_{ts}\right\} = [A_{ts}]\{\dot{e}_{ts}\} \tag{1.35}$$

The material properties for each layer are constant. Hence, the integrals indicated in Eqs. (1.29)-(1.33) are easily evaluated given a chosen stacking sequence.

1.3 Laminate Response in Co-rotational Coordinate System

The isoparametric shell and membrane elements in ADAGIO and PRESTO use a co-rotational coordinate system in order to automatically remove the rigid-body rotations from the deformations before the material model is evaluated. The r-s-t co-rotational system is constructed for each element as follows. The r-direction or material line A corresponds to connecting the midpoints of sides 1-4 and 2-3 as shown in Fig. 1.2. Material line B is constructed by connecting the midpoints of sides 1-2 and 3-4. Because this material direction is not necessarily perpendicular to the first one, it is necessary to construct the s-direction by first finding the t-direction from the cross-product of vectors aligned with material lines A and B. Then, the s-direction results from crossing vectors aligned with the t- and r-directions. It should be obvious that because the s-direction is constructed from the r- and t- directions, it does not track a single material line as an isoparametric element deforms. Hence, the linear elastic material model to be posed in the co-rotational coordinate system will assume that the inplane shear deformations remain small. Furthermore, since the stacking sequence is unknown, the laminate matrices are taken to be constant for all times, as it is not possible to track the fiber orientations of each individual layer. That is, the stacking sequence relative to the r-s-t system is assumed to be constant which is appropriate for small normal and shear strains. Also note that the particular r-s-t system used for an element depends on the ordering of nodes in the element connectivity. Furthermore, the r-s plane is taken to coincide with the element midplane.

It should be apparent that the element co-rotational r-s-t system and the user-defined x-y-z system are not necessarily aligned with each other. Hence, it is necessary to transform the constitutive equations to correspond to the r-s-t system. This transformation is performed internally in the material model initialization coding without any additional user input required. Except in the case of a flat shell, the t-direction will not necessarily be exactly perpendicular to the shell element at its centroid. Recall

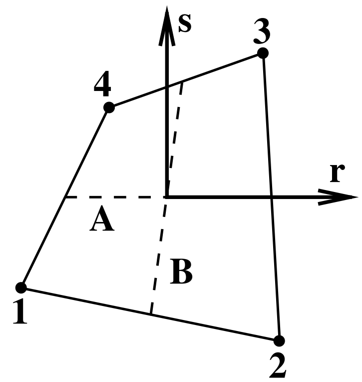

Figure 1.2: Co-rotational coordinate system for a sample element having a connectivity array ordered as {1, 2, 3, 4 }.

that the user-defined system was previously defined to have the z-direction normal to the shell surface. However, an individual x-y-z system is created for each shell element in a mesh as described later in Section 4. Note that in a mesh fine enough for proper finite element convergence, the t- and z-directions for each element should be nearly perpendicular to the shell surface at the element centroid. Let the angle between the r-s-t and x-y-z systems be denoted by θ_2 and positive as shown in Fig. 1.3.

The constitutive equations in the r-s-t system can be determined by applying the appropriate tensor transformations to Eqs. (1.27) and (1.28) to give

$$\begin{Bmatrix} \dot{N}_{rr} \\ \dot{N}_{ss} \\ \dot{N}_{rs} \\ \dot{M}_{rr} \\ \dot{M}_{ss} \\ \dot{M}_{rs} \end{Bmatrix} = \left[\begin{array}{ccc|ccc} \hat{A}_{11} & \hat{A}_{12} & \hat{A}_{16} & \hat{B}_{11} & \hat{B}_{12} & \hat{B}_{16} \\ \hat{A}_{12} & \hat{A}_{22} & \hat{A}_{26} & \hat{B}_{12} & \hat{B}_{22} & \hat{B}_{26} \\ \hat{A}_{16} & \hat{A}_{26} & \hat{A}_{66} & \hat{B}_{16} & \hat{B}_{26} & \hat{B}_{66} \\ \hline \hat{B}_{11} & \hat{B}_{12} & \hat{B}_{16} & \hat{D}_{11} & \hat{D}_{12} & \hat{D}_{16} \\ \hat{B}_{12} & \hat{B}_{22} & \hat{B}_{26} & \hat{D}_{12} & \hat{D}_{22} & \hat{D}_{26} \\ \hat{B}_{16} & \hat{B}_{26} & \hat{B}_{66} & \hat{D}_{16} & \hat{D}_{26} & \hat{D}_{66} \end{array}\right] \begin{Bmatrix} \dot{e}_{rr} \\ \dot{e}_{ss} \\ 2\dot{e}_{rs} \\ \dot{k}_{rr} \\ \dot{k}_{ss} \\ 2\dot{k}_{rs} \end{Bmatrix} - \dot{T} \begin{Bmatrix} \hat{N}^{th}_{rr} \\ \hat{N}^{th}_{ss} \\ \hat{N}^{th}_{rs} \\ \hat{M}^{th}_{rr} \\ \hat{M}^{th}_{ss} \\ \hat{M}^{th}_{rs} \end{Bmatrix} \tag{1.36}$$

and

$$\begin{Bmatrix} \dot{N}_{st} \\ \dot{N}_{tr} \end{Bmatrix} = \begin{bmatrix} \hat{A}_{44} & \hat{A}_{45} \\ \hat{A}_{45} & \hat{A}_{55} \end{bmatrix} \begin{Bmatrix} 2\dot{e}_{st} \\ 2\dot{e}_{tr} \end{Bmatrix} \tag{1.37}$$

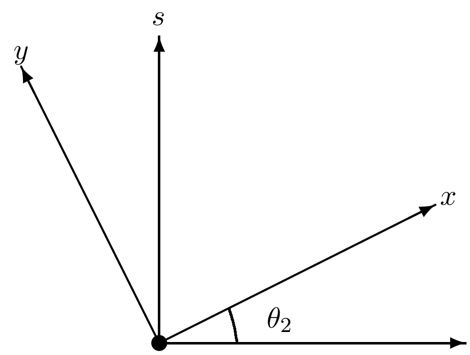

Figure 1.3: Co-rotational (r-s-t) and user-defined (x-y-z) coordinate systems. These systems share a common axis which is (nearly) perpendicular to the shell element at its centroid.

where

$$\left[\hat{A}\right] = [P_1(\theta_2)]^{-1}\,[A]\,[P_1(\theta_2)]^{-T} \tag{1.38}$$

$$\left[\hat{B}\right] = [P_1(\theta_2)]^{-1}\,[B]\,[P_1(\theta_2)]^{-T} \tag{1.39}$$

$$\left[\hat{D}\right] = [P_1(\theta_2)]^{-1}\,[D]\,[P_1(\theta_2)]^{-T} \tag{1.40}$$

$$\left[\hat{A}_{ts}\right] = [P_2(\theta_2)]^{-1}\,[A_{ts}]\,[P_2(\theta_2)]^{-T} \tag{1.41}$$

$$\left\{\hat{N}^{th}\right\} = [P_1(\theta_2)]^{-1}\left\{N^{th}\right\} \tag{1.42}$$

$$\left\{\hat{M}^{th}\right\} = [P_1(\theta_2)]^{-1}\left\{M^{th}\right\} \tag{1.43}$$

In condensed notation, Eqs. (1.36) and (1.37), respectively, are written as

$$\left\{\begin{array}{c}\left\{\dot{\hat{N}}\right\}\\ \left\{\dot{\hat{M}}\right\}\end{array}\right\} = \left[\begin{array}{cc}\left[\hat{A}\right] & \left[\hat{B}\right]\\ \left[\hat{B}\right] & \left[\hat{D}\right]\end{array}\right]\left\{\begin{array}{c}\left\{\dot{\hat{e}}\right\}\\ \left\{\dot{\hat{\kappa}}\right\}\end{array}\right\} - \dot{T}\left\{\begin{array}{c}\left\{\hat{N}^{th}\right\}\\ \left\{\hat{M}^{th}\right\}\end{array}\right\} \tag{1.44}$$

and

$$\left\{\dot{\hat{N}}_{ts}\right\} = \left[\hat{A}_{ts}\right]\left\{\dot{\hat{e}}_{ts}\right\} \tag{1.45}$$

1.4 Strain Kinematics

It is now necessary to relate the total/kinematic strain rates used in Eqs. (1.44) and (1.45) to the nodal degrees-of-freedom. In the r-s-t system for an element, these nodal degrees-of-freedom consist of three translational velocities for the shell midplane (v_r, v_s, and v_t) and two rotational velocities (ω_r and ω_s). The rotational velocities ω_r and ω_s are taken to be positive about the r- and s-axes, respectively. This results in the total translational velocity at any point through the thickness being given by

$$\left\{ \begin{array}{c} V_r(r,s,t) \\ V_s(r,s,t) \\ V_t(r,s,t) \end{array} \right\} = \left\{ \begin{array}{c} v_r(r,s) \\ v_s(r,s) \\ v_t(r,s) \end{array} \right\} + t \left\{ \begin{array}{c} \omega_s(r,s) \\ -\omega_r(r,s) \\ 0 \end{array} \right\} \tag{1.46}$$

The velocity gradient is defined as

$$[l] = \begin{bmatrix} \dfrac{\partial V_r}{\partial r} & \dfrac{\partial V_r}{\partial s} & \dfrac{\partial V_r}{\partial t} \\ \dfrac{\partial V_s}{\partial r} & \dfrac{\partial V_s}{\partial s} & \dfrac{\partial V_s}{\partial t} \\ \dfrac{\partial V_t}{\partial r} & \dfrac{\partial V_t}{\partial s} & \dfrac{\partial V_t}{\partial t} \end{bmatrix} \tag{1.47}$$

Substituting Eq. (1.46) into Eq. (1.47) gives

$$[l] = \begin{bmatrix} v_{r,r} + t\omega_{s,r} & v_{r,s} + t\omega_{s,s} & \omega_s \\ v_{s,r} - t\omega_{r,r} & v_{s,s} - t\omega_{r,s} & -\omega_r \\ v_{t,r} & v_{t,s} & 0 \end{bmatrix} \tag{1.48}$$

where $(\cdot)_{,r} = \partial(\cdot)/\partial r$ and $(\cdot)_{,s} = \partial(\cdot)/\partial s$. The rate-of-deformation tensor is defined as the symmetric part of $[l]$ and is given by

$$[d] = \frac{1}{2}\left([l] + [l]^T\right) \tag{1.49}$$

$$= \begin{bmatrix} d_{rr} & d_{rs} & d_{tr} \\ d_{rs} & d_{ss} & d_{st} \\ d_{tr} & d_{st} & d_{tt} \end{bmatrix} \tag{1.50}$$

with

$$d_{rr} = v_{r,r} + t\omega_{s,r} \tag{1.51}$$

$$d_{ss} = v_{s,s} - t\omega_{r,s} \tag{1.52}$$

$$d_{tt} = 0 \tag{1.53}$$

$$d_{st} = \frac{1}{2}\left(v_{t,s} - \omega_r\right) \tag{1.54}$$

$$d_{tr} = \frac{1}{2}\left(v_{t,r} + \omega_s\right) \tag{1.55}$$

$$d_{rs} = \frac{1}{2}\Big(v_{r,s} + v_{s,r} + t\big(\omega_{s,s} - \omega_{r,r}\big)\Big) \tag{1.56}$$

The co-rotational total strain rates are taken equal to the appropriate rate-of-deformation tensor components such that the midplane strain rates for inplane behavior are given by

$$\left\{ \begin{array}{c} \dot{e}_{rr} \\ \dot{e}_{ss} \\ 2\dot{e}_{rs} \end{array} \right\} = \left\{ \begin{array}{c} v_{r,r} \\ v_{s,s} \\ v_{r,s} + v_{s,r} \end{array} \right\} \tag{1.57}$$

The bending curvature strain rates are expressed as

$$\left\{ \begin{array}{c} \dot{k}_{rr} \\ \dot{k}_{ss} \\ 2\dot{k}_{rs} \end{array} \right\} = \left\{ \begin{array}{c} \omega_{s,r} \\ -\omega_{r,s} \\ \omega_{s,s} - \omega_{r,r} \end{array} \right\} \tag{1.58}$$

Finally, the transverse shear strain rates are determined as

$$\left\{ \begin{array}{c} 2\dot{e}_{st} \\ 2\dot{e}_{tr} \end{array} \right\} = \left\{ \begin{array}{c} v_{t,s} - \omega_r \\ v_{t,r} + \omega_s \end{array} \right\} \tag{1.59}$$

Note that these transverse shear strain rates are constant in the thickness direction and will result in the corresponding transverse shear stresses being constant as well. It is known that modeling both of these as constant results in a transverse shear energy which is too large compared to that coming from a realistic parabolic distribution. Another potential problem that can result from using unmodified shear behavior as given above is that as a shell element becomes thin (small thickness compared to inplane element dimensions), the element may exhibit shear locking. Hence, transverse shear correction factors are used in ADAGIO/PRESTO to achieve better behavior. Because the square root of the transverse shear correction factor is applied to the gradient operator (used to compute the scaled transverse shear strains) and divergence operator (used to compute the element internal forces) outside of the material model coding, the material model itself does not need to apply these shear correction factors in computing the force and force-couple resultants. However, when computing a critical time step for PRESTO, these transverse shear correction factors need to be explicitly taken into account.[1]

2 Numerical Evaluation

Over each time step, the velocity is taken to be constant. However, many choices exist for which configuration to use in evaluating the strain rates which are expressed in terms of the rate-of-deformation tensor. In ADAGIO and PRESTO, the configuration at the middle of the time step is used. Then, the material response is determined as follows:

$$\left\{ \begin{array}{c} \left\{\hat{N}\right\} \\ \left\{\hat{M}\right\} \end{array} \right\}^{n+1} = \left\{ \begin{array}{c} \left\{\hat{N}\right\} \\ \left\{\hat{M}\right\} \end{array} \right\}^{n} + \Delta t^{n+1} \left[\begin{array}{cc} \left[\hat{A}\right] & \left[\hat{B}\right] \\ \left[\hat{B}\right] & \left[\hat{D}\right] \end{array} \right] \left\{ \begin{array}{c} \left\{\dot{\hat{e}}\right\} \\ \left\{\dot{\hat{\kappa}}\right\} \end{array} \right\}^{n+1/2}$$
$$-\Delta T^{n+1} \left\{ \begin{array}{c} \left\{\hat{N}^{th}\right\} \\ \left\{\hat{M}^{th}\right\} \end{array} \right\} \tag{2.1}$$

and

$$\left\{\hat{N}_{ts}\right\}^{n+1} = \left\{\hat{N}_{ts}\right\}^{n} + \Delta t^{n+1} \left[\hat{A}_{ts}\right] \left\{\dot{\hat{e}}_{ts}\right\}^{n+1/2} \tag{2.2}$$

where $\Delta t^{n+1} = t^{n+1} - t^n$ and $\Delta T^{n+1} = T^{n+1} - T^n$. As typically done in ADAGIO/PRESTO, the body is assumed to be stress free at the initial time/temperature, unless explicitly set otherwise.

3 Critical Time Step for Explicit Dynamics

It is well-known that the critical time step for central difference method when applied to linear finite element analysis is determined as[2]

$$\Delta t_{cr} = \frac{2}{\omega_{max}} \tag{3.1}$$

where ω_{max} is the maximum eigenvalue determined from the free vibration of the assembled finite element system. That is, ω_{max} is determined from considering

$$\left| [K] - \omega^2 [M] \right| = 0 \tag{3.2}$$

where $[K]$ and $[M]$ are the assembled stiffness and mass matrices. For nonlinear analysis, the upper limit on the time step necessary to prevent instability is taken to be equal to that computed using Eqs. (3.1) and (3.2) with $[K]$ and $[M]$ evaluated at the start of the time step in question. It can be shown that[2]

$$\omega_{max} \leq \max_{(n)} \omega_{max}^{(n)} \tag{3.3}$$

where $\omega_{max}^{(n)}$ is the maximum frequency of the n^{th} element. Hence, it is sufficient to consider the eigenvalue problem for a single element.

The complete development of the eigenvalue problem for a laminated flat shell is given in Ref. 1. Only the final results of the derivation will be presented here. Note that in determining the critical time step, the thermal force and force-couple resultants from thermal changes can be considered as part of the applied load and hence ignored when considering the free vibration of the assembled finite element system.

The eigenvalue problems are derived by considering a single 4-noded flat bilinear element. When viewed in the plane of the element, each node only has 5 degrees-of-freedom (DOF) (the drilling DOF is missing) for a total of 20 DOF for the element. Using a methodology based on the presented in Refs. 3 and 4, finding the maximum eigenvalue of the resulting (20×20) system is reduced to finding the maximum eigenvalue of an asymmetric (6×6) matrix corresponding to membrane and bending waves which may act in a coupled manner and the maximum eigenvalue of an asymmetric (2×2) matrix corresponding to transverse shear waves. These two eigenvalue problems are uncoupled. The 12 eigenvalues that are eliminated from consideration correspond to rigid body and hourglass modes.

3.1 Eigenvalue Problem Arising From Inplane Stresses

The following (6×6) eigenvalue problem results from the inplane stresses:

$$\left[\begin{array}{c|c} \beta\left[\tilde{A}\right] & \left[\tilde{B}\right] \\ \hline \beta\left[\tilde{B}\right] & \left[\tilde{D}\right] \end{array}\right] \left\{\begin{array}{c} N_{rr}^0 \\ N_{ss}^0 \\ N_{rs}^0 \\ M_{rr}^0 \\ M_{ss}^0 \\ M_{rs}^0 \end{array}\right\} = \frac{\rho A^2 h \beta}{4} \omega^2 \left\{\begin{array}{c} N_{rr}^0 \\ N_{ss}^0 \\ N_{rs}^0 \\ M_{rr}^0 \\ M_{ss}^0 \\ M_{rs}^0 \end{array}\right\} \tag{3.4}$$

where ρ is the material density, A is the element area, β is the rotational inertia scaling factor for a lumped mass matrix and

$$\left[\tilde{A}\right] = \begin{bmatrix} a_{11}\hat{A}_{11} + a_{12}\hat{A}_{16} & a_{22}\hat{A}_{12} + a_{12}\hat{A}_{16} & a_{12}\left(\hat{A}_{11} + \hat{A}_{12}\right) + \left(a_{11} + a_{22}\right)\hat{A}_{16} \\ a_{11}\hat{A}_{12} + a_{12}\hat{A}_{26} & a_{22}\hat{A}_{22} + a_{12}\hat{A}_{26} & a_{12}\left(\hat{A}_{12} + \hat{A}_{22}\right) + \left(a_{11} + a_{22}\right)\hat{A}_{26} \\ a_{11}\hat{A}_{16} + a_{12}\hat{A}_{66} & a_{22}\hat{A}_{26} + a_{12}\hat{A}_{66} & a_{12}\left(\hat{A}_{16} + \hat{A}_{26}\right) + \left(a_{11} + a_{22}\right)\hat{A}_{66} \end{bmatrix} \tag{3.5}$$

with

$$a_{ij} = \{b_i\}^T \{b_j\} \tag{3.6}$$

and

$$\{b_1\}^T = A\frac{\partial \{\Phi\}^T}{\partial r}\bigg|_c = \frac{1}{2}\left\{ \begin{array}{cccc} s_{24} & s_{31} & s_{42} & s_{13} \end{array} \right\} \tag{3.7}$$

$$\{b_2\}^T = A\frac{\partial \{\Phi\}^T}{\partial s}\bigg|_c = \frac{1}{2}\left\{ \begin{array}{cccc} r_{42} & r_{13} & r_{24} & r_{31} \end{array} \right\} \tag{3.8}$$

$$\{b_3\}^T = A\{\Phi\}^T\bigg|_c = \frac{A}{4}\left\{ \begin{array}{cccc} 1 & 1 & 1 & 1 \end{array} \right\} \tag{3.9}$$

where $\{\Phi\}$ is the vector of bilinear shape functions and $|_c$ indicates evaluation at the element centroid. Here r_{ij} is determined in terms of the nodal r_i coordinates as

$$r_{ij} = r_i - r_j \tag{3.10}$$

Similar equations hold for s_{ij}. The element area A is given by

$$A = \frac{1}{2}\left(r_{31}s_{42} + r_{24}s_{31}\right) \tag{3.11}$$

Equations for $\left[\tilde{B}\right]$ and $\left[\tilde{D}\right]$ are obtained by replacing $\hat{A}_{ij}$ by $\hat{B}_{ij}$ and $\hat{D}_{ij}$, respectively, in Eq. (3.5).

Several choices exist for determining the rotational inertia scaling factor β. One possibility is to take β as the ratio of the area moment of inertia to the area as follows:[5]

$$\beta = \frac{I}{A} = \frac{h^2}{12} \tag{3.12}$$

An alternative choice for β is

$$\beta = \frac{A}{12} \tag{3.13}$$

which when multiplied by $\rho A h/4$ gives the mass moment of inertia of one-fourth of a rigid square element. In PRESTO, Eq. (3.13) is used in determining the rotational inertia.

3.2 Eigenvalue Problem Arising from Transverse Shear Stresses

As noted previously, the transverse shear correction factors applied to the gradient and divergence operators must be taken into account for the transverse shear eigenvalue problem. In ADAGIO and PRESTO, separate correction factors denoted by κ_{st} and κ_{tr} are computed for the st and tr transverse shear behaviors as follows:

$$\kappa_{st}^2 = \min\left\{5/6,\ 6h^2/L_{st}^2\right\} \tag{3.14}$$

$$\kappa_{tr}^2 = \min\left\{5/6,\ 6h^2/L_{tr}^2\right\} \tag{3.15}$$

where L_{st} and L_{tr} are characteristic lengths of the element in the s- and r-directions, respectively. A complete discussion of using these shear correction factors is given in Ref. 1. However, for the present discussion, it suffices to point out that 5/6 is the traditional value used to give the same strain energy as a parabolic distribution of transverse shear stresses and strains, whereas the $6h^2/L^2$ value is used to recover Kirchhoff bending behavior for thin shell elements without shear locking the element.

Taking all of this into account, the following (2×2) eigenvalue problem results for transverse shear behavior:

$$\left[\tilde{A}_{ts}\right] \left\{ \begin{array}{c} \kappa_{st} N_{st}^0 \\ \kappa_{tr} N_{tr}^0 \end{array} \right\} = \frac{\rho A^2 h \beta}{4} \omega^2 \left\{ \begin{array}{c} \kappa_{st} N_{st}^0 \\ \kappa_{tr} N_{tr}^0 \end{array} \right\} \tag{3.16}$$

where $\left[\tilde{A}_{ts}\right]$ is a (2×2) matrix given by

$$\left[\tilde{A}_{ts}\right] = \left[\begin{array}{cc} \tilde{A}_{44} & \tilde{A}_{45} \\ \tilde{A}_{54} & \tilde{A}_{55} \end{array} \right] = \left[\begin{array}{c|c} \begin{array}{l} (\beta a_{22} + a_{33})\, \kappa_{st}^2 \hat{A}_{44} \\ +\beta \kappa_{st} \kappa_{tr} a_{12} \hat{A}_{45} \end{array} & \begin{array}{c} \beta \kappa_{st} \kappa_{tr} a_{12} \hat{A}_{44} \\ +\left(\beta a_{11} + a_{33}\right) \kappa_{tr}^2 \hat{A}_{45} \end{array} \\ \hline \begin{array}{l} (\beta a_{22} + a_{33})\, \kappa_{st}^2 \hat{A}_{45} \\ +\beta \kappa_{st} \kappa_{tr} a_{12} \hat{A}_{55} \end{array} & \begin{array}{c} \beta \kappa_{st} \kappa_{tr} a_{12} \hat{A}_{45} \\ +\left(\beta a_{11} + a_{33}\right) \kappa_{tr}^2 \hat{A}_{55} \end{array} \end{array} \right] \tag{3.17}$$

If equal transverse shear factors are applied to both transverse shears ($\kappa_{st} = \kappa_{tr} = \kappa$), the transverse shear eigenvalue problem can be simplified by factoring κ^2 out of $\left[\tilde{A}_{ts}\right]$.

3.3 Critical Time Step Estimation

Obviously, the critical time step is calculated using the maximum of the frequency eigenvalues determined from Eqs. (3.4) and (3.16). Because the geometrical a_{ij} factors change with element deformation, it is necessary at every time step to calculate a value for the critical time step.

In the current implementation in PRESTO, the (2×2) eigenvalue problem for transverse shear given in Eq. (3.16) is solved exactly. On the other hand, the maximum eigenvalue from the (6×6) system given in Eq. (3.4) is only estimated in order to minimize the computational cost. In fact, three independent bounds are computed. The first two bounds correspond to Gerschgorin circles estimates operating on the $(6{\times}6)$ matrix and its transpose. The third bound is determined using the matrix norms induced from L_1 and L_∞ vector norms. Because these three bounds for the maximum membrane/bending frequency are independent, the minimum of these bounds is used as the conservative estimate for the maximum membrane/bending frequency to give an estimated critical time step for membrane/bending behavior which is as large as possible. The final critical time step is the minimum of the those corresponding to membrane/bending and transverse shear waves.

4 Material Orientation Initialization

Although internally the material parameters for each element are transformed to correspond to the element's r-s-t co-rotational coordinate system, the material properties are specified at the material block level on the input deck with respect to a user-defined x-y-z coordinate system.

A general capability for defining rectangular, cylindrical, and spherical coordinate systems is available for the `elastic_laminate` model. In each case, the user-defined coordinate system is created as follows. First, the user inputs three points A, B, and C which define the origin, a point on the user-defined Z'-axis and a point on the user-defined X'-Z' plane, respectively, as shown in Fig. 4.1. Typically, point C is simply given as a point on the user-defined X' axis. Note that for the case of either a cylindrical or spherical coordinate system, point C does not affect the coordinate system definition, except for the reference of where angles in the coordinate system are defined to be zero. That is, the Z'-axis defines the cylindrical and polar axes of cylindrical and spherical systems, respectively. The definition of the X'-Y'-Z' system is general and is given outside of the material block on the ADAGIO/PRESTO input deck.

In order to allow for easier definition of the initial material orientation, additional

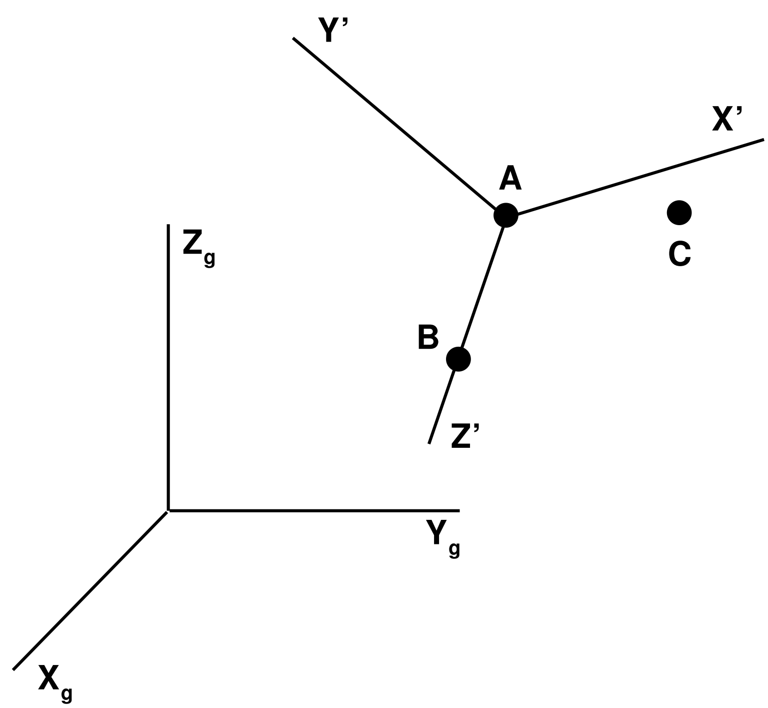

Figure 4.1: User-defined system X'-Y'-Z' specified via points A, B, and C. Also shown is the global X_g-Y_g-Z_g coordinate system.

Table 4.1: Selection of axis of the X''-Y''-Z'' system for projection onto the shell surface. In the event that the first axis chosen for projection is (nearly) perpendicular to the shell surface, the second choice axis becomes the one that is projected.

Axis Chosen for Rotation to Create X''-Y''-Z''	First Choice of Axis to Project onto Surface	Second Choice of Axis to Project onto Surface
X'	Y''	Z''
Y'	X''	Z''
Z'	X''	Y''

manipulations of the user-defined X'-Y'-Z' system are allowed. First, once the X'-Y'-Z' system has been created, the user has the ability to specify a X''-Y''-Z'' system defined by rotating the X'-Y'-Z' system by angle α about one of its coordinate axes as shown in Fig. 4.2. For many curved shell structures, it is unlikely that the shell surface is always parallel to any one of the axes of the X''-Y''-Z'' system. Hence, it is necessary to project one of these axes onto the shell surface. The axis chosen for projection is the selected as follows. First, the axis used to create the X''-Y''-Z'' system by rotating the X'-Y'-Z' system is eliminated from consideration. Of the remaining two axes, the one chosen is the alphabetically first axis that has a non-zero projection. This selection procedure is explicitly given in Table 4.1. For example, if the X''-Y''-Z'' system is created by rotating the X'-Y'-Z' system about the Y'-axis, the X''-axis will be the one projected, unless its projection is (nearly) zero in which case the Z''-axis will be projected instead.

After this projection operation, the user-defined system is known in terms of the projected axis and the element normal. The user is allowed one final manipulation which is to rotate the resulting system by angle θ about the element normal to give the final x-y-z system used in specifying the material properties as shown in Fig. 4.3. The first direction corresponds to the rotated projected axis, while the third direction is aligned with the element normal and the second direction completes the right-handed system. The material parameters are then specified by the user with respect to this x-y-z coordinate system.

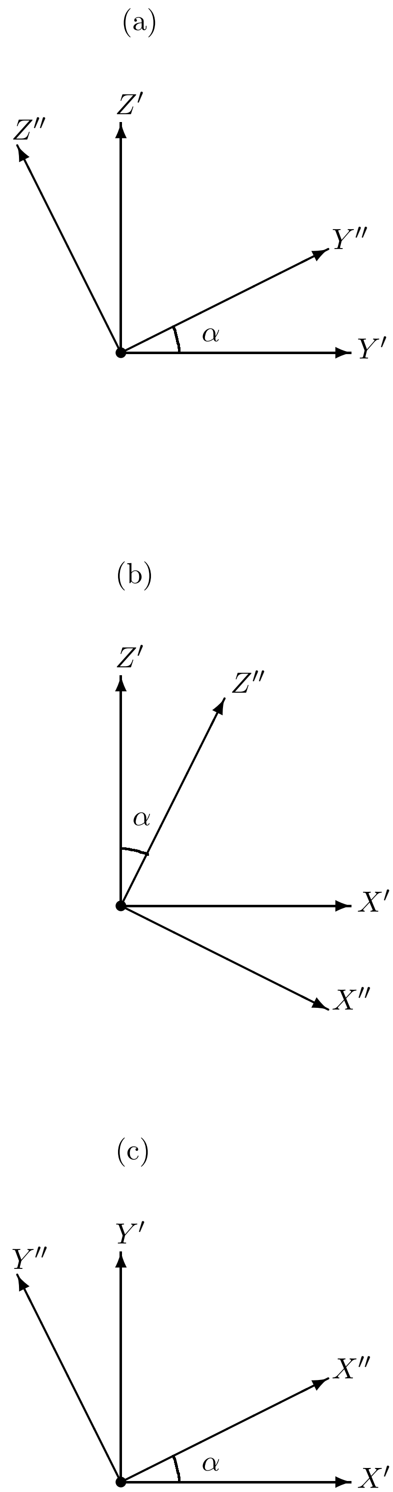

Figure 4.2: Creation of X''-Y''-Z'' coordinate system by rotation of the X'-Y'-Z' system about one its axes by angle α: (a) rotation about X'; (b) rotation about Y'; (c) rotation about Z'.

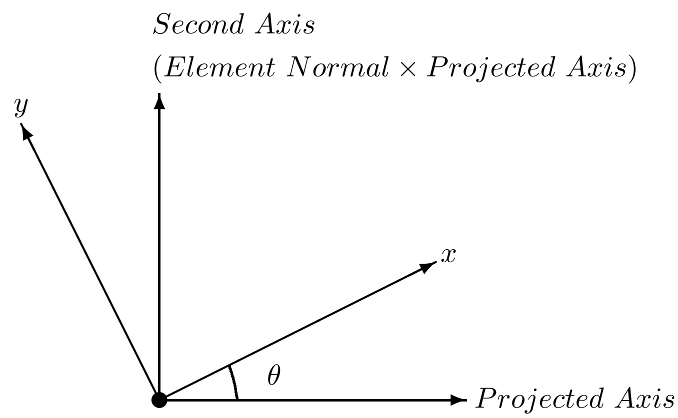

Figure 4.3: Creation of x-y-z coordinate system by rotation of the projected system by angle θ about the element normal.

In summary, the x-y-z system is created individually for each element as follows. First the user inputs three points defining the X'-Y'-Z' system. The user also specifies whether the X'-Y'-Z' is a rectangular, cylindrical, or spherical coordinate system. For cylindrical and spherical systems, the global directions of X'-, Y'-, and Z'-axes depend upon the location of the centroid of the element in question. Next, the X''-Y''-Z'' system is created by rotating the X'-Y'-Z' system about one of its axis by a user-defined angle α. After this, one of the axes of the X''-Y''-Z'' system is projected onto the element surface. The resulting coordinate system is rotated about the element normal by user-specified angle θ to give the final x-y-z system.

5 Stress Output

Although layer information must be known to generate appropriate values for $[A]$, $[A_{ts}]$, $[B]$, and $[D]$, this layer information is not used inside either ADAGIO or PRESTO and, hence, is not specified on the input deck. Therefore, it is not possible for either code to generate layer stresses corresponding to the actual layer properties. Nevertheless, an equivalent linear stress distribution through the thickness is computed. When this equivalent stress variation is integrated through the thickness it gives the same force and force-couple resultants as the actual laminate lay-up.

The equivalent stress distribution is shown in Fig. 5.1 and is given in terms of the average stress $\bar{\sigma}_{ij}$ and $\delta\sigma_{ij}$ which is one-half the total stress variation through the

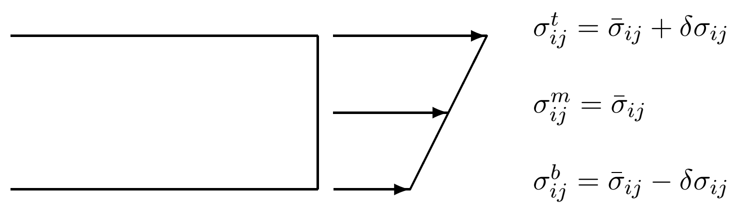

Figure 5.1: Equivalent linear stress distribution through the laminate thickness. The values at the bottom, middle, and top are marked.

thickness. Equating the force and force-couple resultants coming from the equivalent stress distribution to those from the unknown real stress distribution, the average stress and stress variation are given by

$$\bar{\sigma}_{ij} = \frac{N_{ij}}{h} \tag{5.1}$$

and

$$\delta\sigma_{ij} = \frac{6}{h^2} M_{ij} \tag{5.2}$$

The resulting values of the equivalent stress at the bottom, middle, and top are then

$$\sigma_{ij}^b = \frac{N_{ij}}{h} - \frac{6}{h^2} M_{ij} \tag{5.3}$$

$$\sigma_{ij}^m = \frac{N_{ij}}{h} \tag{5.4}$$

$$\sigma_{ij}^t = \frac{N_{ij}}{h} + \frac{6}{h^2} M_{ij} \tag{5.5}$$

Because the middle stress is equal to the average stress, it is reported as the "membrane" stress value. The stress values reported on output are given with respect to the global coordinate system.

6 ADAGIO/PRESTO Input and Output Keywords

Sample input decks for several problems discussed in the next section are given in the Appendices. Here, the keywords needed to use the elastic laminate model will be defined.

6.1 Definition of X'-Y'-Z' System

Points A, B, and C that define the X'-Y'-Z' are input using the following syntax:

```
DEFINE POINT <string>point_name
      WITH COORDINATES <real>Xg_value <real>Yg_value <real>Zg_value
```

The X'-Y'-Z' coordinate system is then defined as follows:

```
DEFINE COORDINATE SYSTEM <string>coord_sys_name
      <string>RECTANGULAR|CYLINDRICAL|SPHERICAL
      WITH POINT <string>ptA_name POINT<string>ptB_name
      POINT<string>ptC_name
```

The completion of the user-defined x-y-z system used for input of material properties is completed in the model definition block by specifying angles α and θ and the axis about which the α rotation is to be applied.

6.2 Elastic Laminate Model Definition

Parameters for the elastic laminate material model are given using the following input syntax:

```
BEGIN PARAMETERS FOR MODEL ELASTIC_LAMINATE
  A11 = <real>a11_value
  A12 = <real>a12_value
  A16 = <real>a16_value
  A22 = <real>a22_value
  A26 = <real>a26_value
  A66 = <real>a66_value
  A44 = <real>a44_value
  A45 = <real>a45_value
  A55 = <real>a55_value
  B11 = <real>b11_value
  B12 = <real>b12_value
  B16 = <real>b16_value
  B22 = <real>b22_value
```

```
  B26 = <real>b26_value
  B66 = <real>b66_value
  D11 = <real>d11_value
  D12 = <real>d12_value
  D16 = <real>d16_value
  D22 = <real>d22_value
  D26 = <real>d26_value
  D66 = <real>d66_value
  COORDINATE SYSTEM = <string>coord_sys_name
  DIRECTION FOR ROTATION = 1|2|3
  ALPHA = <real>alpha_value
  THETA = <real>theta_value
  NTH11 FUNCTION = <string>nth11_function_name
  NTH22 FUNCTION = <string>nth22_function_name
  NTH12 FUNCTION = <string>nth12_function_name
  MTH11 FUNCTION = <string>mth11_function_name
  MTH22 FUNCTION = <string>mth22_function_name
  MTH12 FUNCTION = <string>mth12_function_name
END PARAMETERS FOR MODEL ELASTIC_LAMINATE
```

The values for A_{ij}, B_{ij}, D_{ij}, N_{ij}^{th}, and M_{ij}^{th} are given with respect to the x-y-z coordinate system created for each element as previously explained. Note that both `alpha_value` and `theta_value` in the user coordinate system definition are given in degrees. The user is required to ensure that all of the material parameters are consistent with the chosen laminate stacking sequence, as no such explicit checking is performed in the code.

Here the `NTHIJ` and `MTHIJ FUNCTION`'s specify the components of the relative thermal force and force-couple resultants at a given temperature. That is, these functions are populated with values determined using

$$\texttt{NTHIJ FUNCTION} \text{ value at } T = (T - T_{ref})N_{ij}^{th} \tag{6.1}$$

$$\texttt{MTHIJ FUNCTION} \text{ value at } T = (T - T_{ref})M_{ij}^{th} \tag{6.2}$$

where T_{ref} is the temperature at which the thermal force and force-couple resultants are defined to be zero.

The model was implemented such that when thermal strains are to be included, not only must nonzero functions be specified for the thermal force and force-couple resultants, but the `THERMALSTRAIN` option must be given in the ADAGIO region definition as follows:

```
OPTIONS = THERMALSTRAIN
```

If this option is not given, then the thermal force and force-couple resultants will be set to zero regardless of the values specified in their respective functions. This choice was made to allow thermal strains to be turned-on and off easily without having to change function definitions.

6.3 Output of Relevant Results

A number of results variables are available for this model. Some of these variables are specific to the `elastic_laminate` model, while others are general variables available for all shell/membrane material models. Accessing some of the most useful variables is achieved by giving the following commands in the results output block of the ADAGIO/PRESTO region:

```
ELEMENT VARIABLES = BOTTOM_STRESS
ELEMENT VARIABLES = MEMBRANE_STRESS
ELEMENT VARIABLES = TOP_STRESS
ELEMENT VARIABLES = AR
ELEMENT VARIABLES = AS
ELEMENT VARIABLES = AXIS1_DIR
ELEMENT VARIABLES = AXIS2_DIR
ELEMENT VARIABLES = ELEMENT_THICKNESS
ELEMENT VARIABLES = ELEMENT_AREA
```

Here the stress variables that are output for the `elastic_laminate` model are as defined in Section 5. Recall, these stresses are output in component form using the global coordinate system. The variables `AR` and `AS` give the direction cosines of the user-defined x-axis relative the r- and s-axes of the co-rotational system, respectively. The global direction cosines of the user-defined x- and y-axes are, respectively, given in variables `AXIS1_DIR` and `AXIS2_DIR`. Variables `ELEMENT_THICKNESS` and `ELEMENT_AREA` are self-explanatory.

7 Verification Examples

Although a dozen or more verification tests have been implemented as SIERRA regression tests, only a couple of the examples will be presented here. In each case, the analysis problem will be described and comparison of the numerical results to analytic solutions will be presented. The input decks for these examples are included in the Appendices.

7.1 Fully Constrained Laminated Plate Under Thermal Loading

A 1" x 1" plate which is 0.04" thick is subjected to a 100°F temperature change. The plate is initially stress free at the initial temperature of 82°F. This initial temperature is different than the temperature at which the thermal force and force-couple resultants are chosen to be zero. This reference temperature for zero thermal force and force-couple resultants is specified as 72°F. The square plate has its edges aligned with the global coordinate directions with its thickness in the Z_g-direction. All edges are fully constrained with no displacements or rotations allowed.

The laminate is composed of layers of a contrived orthotropic material having the following properties:

$$E_1 = 7.8 \times 10^6 \text{ psi} \tag{7.1}$$

$$E_2 = 2.6 \times 10^6 \text{ psi} \tag{7.2}$$

$$\nu_{12} = 0.25 \tag{7.3}$$

$$G_{12} = 1.25 \times 10^6 \text{ psi} \tag{7.4}$$

$$G_{23} = G_{12} \tag{7.5}$$

$$G_{31} = G_{12} \tag{7.6}$$

$$\alpha_1 = 3.5 \times 10^{-6} \text{ /°F} \tag{7.7}$$

$$\alpha_2 = 11.4 \times 10^{-6} \text{ /°F} \tag{7.8}$$

A stacking sequence of $[20/40/-15/-30]$ relative to the X_g-axis of the global coordinate system is used with each of the four layers having a thickness of 0.01. Relative to the global coordinate system, the laminate has the following laminate matrices:

$$\begin{bmatrix} A_{11} & A_{12} & A_{16} \\ A_{12} & A_{22} & A_{26} \\ A_{16} & A_{26} & A_{66} \end{bmatrix} = \begin{bmatrix} 248.07 & 52.1327 & 1.29792 \\ 52.1327 & 125.622 & 5.6476 \\ 1.29792 & 5.6476 & 75.5795 \end{bmatrix} \times 10^3 \text{ lb/in} \tag{7.9}$$

$$\begin{bmatrix} B_{11} & B_{12} & B_{16} \\ B_{12} & B_{22} & B_{26} \\ B_{16} & B_{26} & B_{66} \end{bmatrix} = \begin{bmatrix} -29.6388 & 15.598 & -580.464 \\ 15.598 & -1.55715 & -217.625 \\ -580.464 & -217.625 & 15.598 \end{bmatrix} \text{ lb} \tag{7.10}$$

$$\begin{bmatrix} D_{11} & D_{12} & D_{16} \\ D_{12} & D_{22} & D_{26} \\ D_{16} & D_{26} & D_{66} \end{bmatrix} = \begin{bmatrix} 33.7379 & 6.89019 & -0.422002 \\ 6.89019 & 16.2093 & -0.532016 \\ -0.422002 & -0.532016 & 10.0164 \end{bmatrix} \text{ lb} \cdot \text{in} \tag{7.11}$$

$$\begin{bmatrix} A_{44} & A_{45} \\ A_{45} & A_{55} \end{bmatrix} = \begin{bmatrix} 50.0 & 0.0 \\ 0.0 & 50.0 \end{bmatrix} \times 10^3 \text{ lb/in} \tag{7.12}$$

with the following nominal thermal force and force-couple resultants

$$\begin{Bmatrix} N_{11}^{th} \\ N_{22}^{th} \\ N_{12}^{th} \end{Bmatrix} = \begin{Bmatrix} 1.39376 \\ 1.32794 \\ 0.00373322 \end{Bmatrix} \text{(lb/in)/}^\circ\text{F} \tag{7.13}$$

$$\begin{Bmatrix} M_{11}^{th} \\ M_{22}^{th} \\ M_{12}^{th} \end{Bmatrix} = \begin{Bmatrix} -7.54694 \times 10^{-6} \\ 7.54694 \times 10^{-6} \\ -0.000428973 \end{Bmatrix} \text{lb/}^\circ\text{F} \tag{7.14}$$

In order to demonstrate the use of the user-defined coordinate system, the material properties are actually input relative to a coordinate system which is created as the global coordinate system rotated by 15° about the Z_g-axis. Relative to this coordinate system, the laminate has a stacking sequence of $[5/25/-30/-45]$. The laminate properties relative to this coordinate system are

$$\begin{bmatrix} A_{11} & A_{12} & A_{16} \\ A_{12} & A_{22} & A_{26} \\ A_{16} & A_{26} & A_{66} \end{bmatrix} = \begin{bmatrix} 243.513 & 51.9604 & -9.82541 \\ 51.9604 & 130.524 & -14.7717 \\ -9.82541 & -14.7717 & 75.4072 \end{bmatrix} \times 10^3 \text{ lb/in} \tag{7.15}$$

$$\begin{bmatrix} B_{11} & B_{12} & B_{16} \\ B_{12} & B_{22} & B_{26} \\ B_{16} & B_{26} & B_{66} \end{bmatrix} = \begin{bmatrix} -576.117 & 164.913 & -419.274 \\ 164.913 & 246.291 & -264.871 \\ -419.274 & -264.871 & 164.913 \end{bmatrix} \text{ lb} \tag{7.16}$$

$$\begin{bmatrix} D_{11} & D_{12} & D_{16} \\ D_{12} & D_{22} & D_{26} \\ D_{16} & D_{26} & D_{66} \end{bmatrix} = \begin{bmatrix} 32.3781 & 6.59888 & -2.15462 \\ 6.59888 & 18.1518 & -3.05374 \\ -2.15462 & -3.05374 & 9.72512 \end{bmatrix} \text{ lb} \cdot \text{in} \tag{7.17}$$

$$\begin{bmatrix} A_{44} & A_{45} \\ A_{45} & A_{55} \end{bmatrix} = \begin{bmatrix} 50.0 & 0.0 \\ 0.0 & 50.0 \end{bmatrix} \times 10^3 \text{ lb/in} \tag{7.18}$$

and the corresponding nominal thermal force and force-couple resultants are

$$\begin{Bmatrix} N_{11}^{th} \\ N_{22}^{th} \\ N_{12}^{th} \end{Bmatrix} = \begin{Bmatrix} 1.39122 \\ 1.33049 \\ -0.0132209 \end{Bmatrix} (\text{lb/in})/^\circ\text{F} \tag{7.19}$$

$$\begin{Bmatrix} M_{11}^{th} \\ M_{22}^{th} \\ M_{12}^{th} \end{Bmatrix} = \begin{Bmatrix} -0.000221022 \\ 0.000221022 \\ -0.000367728 \end{Bmatrix} \text{lb}/^\circ\text{F} \tag{7.20}$$

Because the plate is constrained along all of its edges, the kinematic strains are zero and the following force and force-couple resultants are obtained:

$$\{N\} = -\Delta T \left\{N^{th}\right\} \tag{7.21}$$

$$\{M\} = -\Delta T \left\{M^{th}\right\} \tag{7.22}$$

The results computed using a single element in ADAGIO are compared to the analytic results in Table 7.1. Excellent agreement is achieved, as expected for such a straightforward analysis.

Table 7.1: Analytic and numerical results for global stress components of a fully constrained laminated plate under thermal loading.

Result	Analytic (psi)	ADAGIO (psi)
σ^b_{XX}	-3487.23	-3487.23
σ^m_{XX}	-3484.40	-3484.40
σ^t_{XX}	-3481.57	-3481.57
σ^b_{YY}	-3317.03	-3317.02
σ^m_{YY}	-3319.86	-3319.85
σ^t_{YY}	-3322.69	-3322.68
σ^b_{XY}	-170.198	-170.2009
σ^m_{XY}	-9.33304	-9.336119
σ^t_{XY}	151.532	151.5287

7.2 Antisymmetric Angle-Ply Plate Under Uniform Pressure

A rectangular antisymmetric angle-ply laminated plate is subjected to a uniform pressure load of $q = 0.003$ psi. The plate has its edges aligned with the global directions and measures 12.0×8.0 in. in the X_g- and Y_g-directions. The plate is simply supported on each edge. The antisymmetric angle-ply stacking sequence is $[\mp 30_2]_A = [-30/30/-30/30/-30/30/-30/30]$. A thickness of 0.01 in. is used for each of the eight layers.

The following properties corresponding to T300/5208 Gr/Ep are used:

$$E_1 = 26.25 \times 10^6 \text{ psi} \tag{7.23}$$

$$E_2 = 1.49 \times 10^6 \text{ psi} \tag{7.24}$$

$$\nu_{12} = 0.28 \tag{7.25}$$

$$G_{12} = 1.04 \times 10^6 \text{ psi} \tag{7.26}$$

$$G_{23} = G_{12} \tag{7.27}$$

$$G_{31} = G_{12} \tag{7.28}$$

For this verification example, the user-defined x-y-z coordinate system for material parameter input is identical to the global coordinate system.

A closed-form solution is developed using classical lamination theory including application of the Kirchhoff condition of zero transverse shear strains. Denoting the inplane displacements in the x and y directions by u and v and the transverse deflection by w, the governing equations for a flat laminated plate under pressure are

$$A_{11}u_{,xx} + A_{66}u_{,yy} + (A_{12} + A_{66})v_{,xy} - 3B_{16}w_{,xxy} - B_{26}w_{,yyy} = 0 \tag{7.29}$$

$$(A_{12} + A_{66})u_{,xy} + A_{66}v_{,xx} + A_{22}v_{,yy} - B_{16}w_{,xxx} - 3B_{26}w_{,xyy} = 0 \tag{7.30}$$

$$\begin{aligned} D_{11}w_{,xxxx} + 2(D_{12} + 2D_{66})w_{,xxyy} + D_{22}w_{,yyyy} \\ -B_{16}(3u_{,xxy} + v_{,xxx}) - B_{26}(u_{,yyy} + 3v_{,xyy}) &= q \end{aligned} \tag{7.31}$$

where A_{ij}, B_{ij}, and D_{ij} denote laminate stiffnesses and $(\cdot)_{,x}$ and $(\cdot)_{,y}$ denote spatial derivatives.

The simply supported boundary conditions are chosen as

$$x = 0, a: \quad u = 0 \tag{7.32}$$
$$w = 0 \tag{7.33}$$
$$N_{xy} = 0 \tag{7.34}$$
$$M_{xx} = 0 \tag{7.35}$$

and

$$y = 0, b: \quad v = 0 \tag{7.36}$$
$$w = 0 \tag{7.37}$$
$$N_{xy} = 0 \tag{7.38}$$
$$M_{yy} = 0 \tag{7.39}$$

where a and b are plate lengths along the x- and y-directions, respectively, and N_{ij} and M_{ij} are the usual force and force-couple resultants, respectively. Using the constitutive law, the strain-displacement relations, and the conditions on u, v, and w given above, the boundary conditions can be written strictly in terms of the the displacements and their derivatives as

$$x = 0, a: \quad u = 0 \tag{7.40}$$
$$w = 0 \tag{7.41}$$
$$v_{,x} = 0 \tag{7.42}$$
$$w_{,xx} = 0 \tag{7.43}$$

and

$$y = 0, b: \quad v = 0 \tag{7.44}$$

$$w = 0 \tag{7.45}$$

$$u_{,y} = 0 \tag{7.46}$$

$$w_{,yy} = 0 \tag{7.47}$$

The uniform pressure load can be written as a Fourier series as follows:

$$q = \sum_{m=1,3,5}^{\infty} \sum_{n=1,3,5}^{\infty} \frac{16q_0}{\pi^2 mn} \sin\frac{m\pi x}{a} \sin\frac{n\pi y}{b} \tag{7.48}$$

where q_0 is the pressure magnitude.

The governing equations and boundary conditions are satisfied exactly by choosing

$$u = \sum_{m=1,3,5}^{\infty} \sum_{n=1,3,5}^{\infty} I_{mn} \sin\frac{m\pi x}{a} \cos\frac{n\pi y}{b} \tag{7.49}$$

$$v = \sum_{m=1,3,5}^{\infty} \sum_{n=1,3,5}^{\infty} J_{mn} \cos\frac{m\pi x}{a} \sin\frac{n\pi y}{b} \tag{7.50}$$

$$w = \sum_{m=1,3,5}^{\infty} \sum_{n=1,3,5}^{\infty} K_{mn} \sin\frac{m\pi x}{a} \sin\frac{n\pi y}{b} \tag{7.51}$$

The I_{mn}, J_{mn} and K_{mn} coefficients are determined by substituting Eqs. (7.48)-(7.51) into Eqs. (7.29)-(7.31) and solving.

In the finite element solution, the quarter of the panel for which $0 \leq x \leq a/2$ and $0 \leq y \leq b/2$ is modeled with symmetry boundary conditions enforced on the two edges $x = a/2$ and $y = b/2$. The essential or kinematic boundary conditions to be applied in determining the finite element solution are

$$x = 0: \quad u = 0, \quad w = 0 \tag{7.52}$$

$$y = 0: \quad v = 0, \quad w = 0 \tag{7.53}$$

$$x = a/2: \quad u = 0, \quad \theta_y = \theta_z = 0 \tag{7.54}$$

$$y = b/2: \quad v = 0, \quad \theta_x = \theta_z = 0 \tag{7.55}$$

The spatial discretization uses a total of 260 elements and 294 nodes. The input deck listing in Appendix B shows how to use the full tangent preconditioner in conjunction with the FETI linear solver for the conjugate gradient solution method employed by ADAGIO. The `shell drilling stiffness` is an adjustable parameter used to create a positive definite matrix for the linear solver. Although more costly than a

Table 7.2: Analytic and numerical results for transverse deflection at center of anti-symmetric angle-ply plate under uniform pressure.

Analytic I (in)*	Analytic II (in)+	ADAGIO (in)
0.000238069	0.000238099	0.000237272

*using $m = 1, 3, 5, 7$ and $n = 1, 3, 5, 7$

+using $m = 1, 3, \ldots, 19$ and $n = 1, 3, \ldots, 19$

nodal preconditioner, the full tangent preconditioner allows the solution of a broader range of composite problems than does the nodal preconditioner. In fact, for this particular problem, convergence was not achieved for several options tried with the nodal preconditioner.

The analytical and numerical results for the midpoint transverse deflection are given in Table 7.2. Note that using 100 terms in the Fourier series expansion gives converged analytical results, as using 100 terms gives a midpoint deflection value that is only 0.0126% different from that computed using 16 terms. Shown in Figs. 7.1 and 7.2 are results for the transverse deflection along the lines $x = a/2$ and $y = b/2$, respectively. Because the response is symmetric, only one-half of the centerline results are shown. In these figures, the analytic results correspond to using $m = 1, 3, \ldots, 19$ and $n = 1, 3, \ldots, 19$. The numerical and analytical results are in excellent agreement.

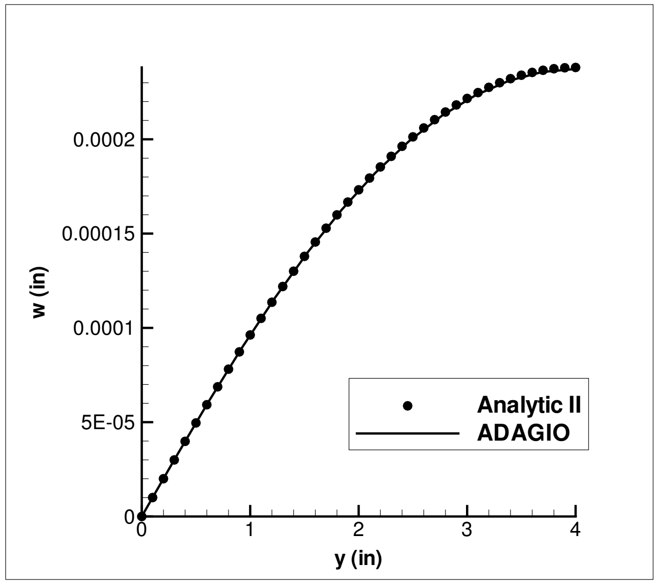

Figure 7.1: Transverse deflection of antisymmetric angle-ply plate along the $x = a/2$ centerline.

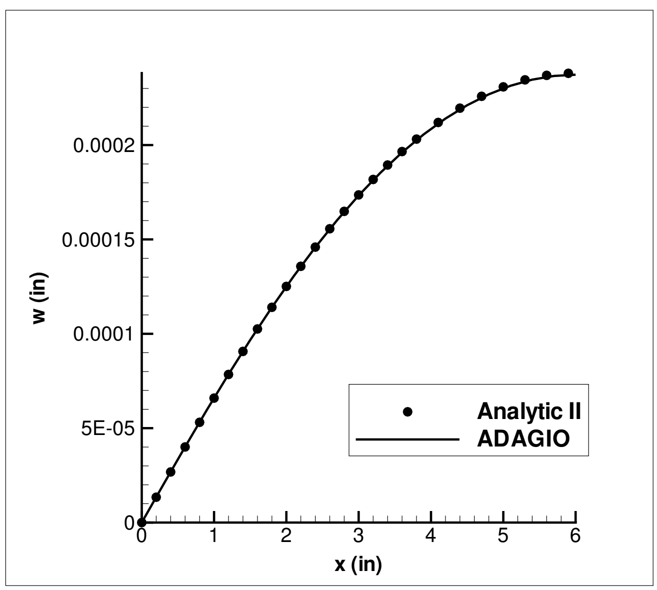

Figure 7.2: Transverse deflection of antisymmetric angle-ply plate along the $y = b/2$ centerline.

7.3 Cross-Ply Cylindrical Panel Under Uniform Pressure

A cylindrical panel is subjected to a uniform pressure load of $q_3 = 0.003$ psi. The pressure is applied on the concave side of the panel pointing away from the center of curvature of the panel cross sections. The length of the panel is 80 in., while the arc length of the other side is 41.89 in. corresponding to a half-angle of $\phi = 12°$ and a radius of 100 in. On each edge, the cylindrical panel rests on diaphragms which are rigid in their plane, but perfectly flexible otherwise. These diaphragms are perpendicular to the panel surface along its edges. The symmetric cross-ply stacking sequence is $[0/90]_S = [0/90/90/0]$ with the thickness of each layer taken to be 0.08 in., giving a total laminate thickness of 0.32 in.

The following properties corresponding to a graphite epoxy are used for each layer:

$$E_1 = 18 \times 10^6 \text{ psi} \tag{7.56}$$

$$E_2 = 1.4 \times 10^6 \text{ psi} \tag{7.57}$$

$$\nu_{12} = 0.34 \tag{7.58}$$

$$G_{12} = 0.9 \times 10^6 \text{ psi} \tag{7.59}$$

$$G_{23} = 10^7 \text{ psi} \tag{7.60}$$

$$G_{31} = 10^7 \text{ psi} \tag{7.61}$$

A closed-form solution for this problem using shallow shell theory is computed as follows. Consider the curvilinear shell coordinate system to be as shown in Fig. 7.3a. The first shell coordinate ξ_1 varies along the direction having zero curvature, while the second shell coordinate ξ_2 varies along the direction having constant non-zero curvature. The third shell coordinate ξ_3 (the shell normal) is determined from the right-hand rule and points away from the center of curvature of the ξ_1-constant arcs. As chosen, the shell coordinates are principal coordinates.

The symmetric cross-ply stacking sequence $[0/90]_S$ has the fibers in the 0° layers aligned with the ξ_1-axis, whereas the 90° layers have fibers aligned with the ξ_2-axis. The laminate matrices are input into ADAGIO relative to a user-defined cylindrical system created in a way such that the user-defined x-axis is aligned with ξ_1-axis and the user-defined y-axis is aligned with the ξ_2-axis. This user-defined cylindrical system is defined as shown in Appendix C. The origin of this system is chosen as the center of curvature of the $\xi_1 = 0$ ($X_g = 0$) edge. The second point which along with the origin defines the cylindrical axis is determined by adding ΔX_g to the global coordinates of the origin of the cylindrical system. Using this construction with the Z'-axis chosen as the axis of rotation to create the X''-Y''-Z'' system with $\alpha = 0$, the Y'' axis of the X''-Y''-Z'' system is projected onto the shell surface to give an axis aligned in the negative ξ_2-direction. Hence, an additional rotation of $\theta = 90°$ is applied about the shell normal to give the user-defined x-axis aligned with ξ_1.

Let v_1, v_2, and v_3 be the translational displacements in the directions of the three shell coordinates. Using the Love-Kirchhoff hypothesis and other approximations appropriate for thin elastic laminated shallow shells as described by Leissa and Qatu[6] the governing equations in terms of v_1, v_2, and v_3 for a shallow elastic cylindrical panel with a symmetric cross-ply stacking sequence under uniform pressure are

$$A_{11}\, v_{1,11} + A_{12}\left(v_{2,12} + \frac{v_{3,1}}{R_2}\right) + A_{66}\,(v_{1,22} + v_{2,12}) \quad = \quad 0 \tag{7.62}$$

$$A_{12}\, v_{1,12} + A_{22}\left(v_{2,22} + \frac{v_{3,2}}{R_2}\right) + A_{66}\,(v_{1,12} + v_{2,11}) \quad = \quad 0 \tag{7.63}$$

$$\begin{aligned} A_{12}\,\frac{v_{1,1}}{R_2} + A_{22}\left(\frac{v_{2,2}}{R_2} + \frac{v_3}{R_2^2}\right) + D_{11}\, v_{3,1111} & \\ +2(D_{12} + 2D_{66})\, v_{3,1122} + D_{22}\, v_{3,2222} \quad &= \quad q_3 \end{aligned} \tag{7.64}$$

Here R_2 is the radius associated with the panel and $(\cdot)_{,i}$ denotes differentiation with respect to shell coordinate ξ_i.

The uniform pressure load q_3 is written as

$$q_3 = \sum_{m=1,3,5}^{\infty} \sum_{n=1,3,5}^{\infty} \frac{16 q_0}{\pi^2 mn} \sin\frac{m\pi\xi_1}{l_1} \sin\frac{n\pi\xi_2}{l_2} \tag{7.65}$$

where the magnitude is denoted by q_0. The boundary conditions are

$$\xi_1 = 0,\, l_1: \qquad v_2 = v_3 = 0 \quad \text{and} \quad N_{11} = 0,\ M_{11} = 0 \tag{7.66}$$

$$\xi_2 = 0,\, l_2: \qquad v_1 = v_3 = 0 \quad \text{and} \quad N_{22} = 0,\ M_{22} = 0 \tag{7.67}$$

where N_{ij} and M_{ij} are the usual force and force-couple resultants in the directions of the shell coordinates. Using the constitutive law, the strain-displacement relations, and the conditions on v_1-v_3 given above, the boundary conditions can be written

(a)

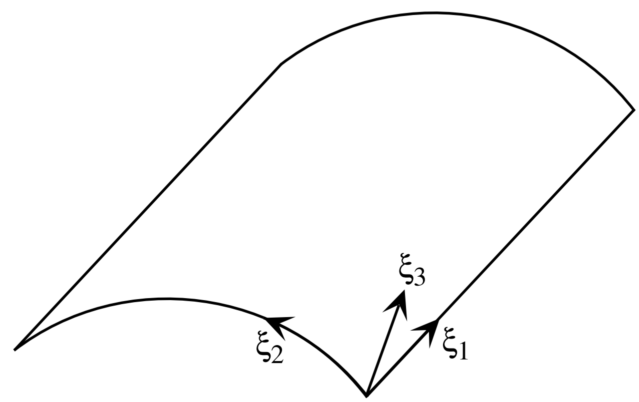

(b)

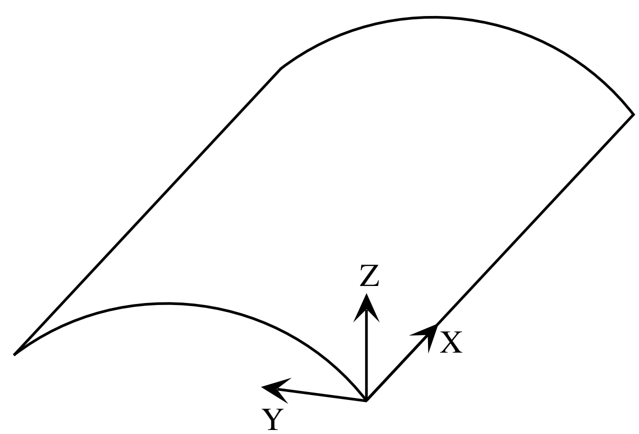

Figure 7.3: Coordinate systems for cylindrical panel under uniform pressure: (a) shell coordinate system; (b) global X-Y-Z (X_g-Y_g-Z_g) coordinate system.

strictly in terms of v_1-v_3 as

$$\xi_1 = 0,\, l_1: \qquad v_2 = v_3 = 0 \quad \text{and} \quad v_{1,1} = 0,\; v_{3,11} = 0 \tag{7.68}$$

$$\xi_2 = 0,\, l_2: \qquad v_1 = v_3 = 0 \quad \text{and} \quad v_{2,2} = 0,\; v_{3,22} = 0 \tag{7.69}$$

The boundary conditions and governing equations are satisfied exactly by the following Fourier series expansions:

$$v_1 = \sum_{m=1,3,5}^{\infty} \sum_{n=1,3,5}^{\infty} I_{mn} \cos\frac{m\pi\xi_1}{l_1} \sin\frac{n\pi\xi_2}{l_2} \tag{7.70}$$

$$v_2 = \sum_{m=1,3,5}^{\infty} \sum_{n=1,3,5}^{\infty} J_{mn} \sin\frac{m\pi\xi_1}{l_1} \cos\frac{n\pi\xi_2}{l_2} \tag{7.71}$$

$$v_3 = \sum_{m=1,3,5}^{\infty} \sum_{n=1,3,5}^{\infty} K_{mn} \sin\frac{m\pi\xi_1}{l_1} \sin\frac{n\pi\xi_2}{l_2} \tag{7.72}$$

The constant coefficients I_{mn}, J_{mn}, and K_{mn} are determined by substituting Eqs. (7.70)-(7.72) into Eqs. (7.62)-(7.64) and solving.

In the finite element solution, the quarter of the panel for which $l_1/2 \leq \xi_1 \leq l_1$ and $l_2/2 \leq \xi_2 \leq l_2$ is modeled with symmetry boundary conditions enforced on the two edges $\xi_1 = l_1/2$ and $\xi_2 = l_2/2$. The global coordinate system for the finite element analysis is shown in Fig. 7.3b. The geometric or essential boundary conditions to be applied in the finite element solution are

$$\xi_1 = l_1/2: \qquad u = 0,\; \theta_y = \theta_z = 0 \tag{7.73}$$

$$\xi_2 = l_2/2: \qquad v = 0,\; \theta_x = \theta_z = 0 \tag{7.74}$$

$$\xi_1 = l_1: \qquad v = w = 0 \tag{7.75}$$

$$\xi_2 = l_2: \qquad u = 0,\; w\cos\phi + v\sin\phi = 0 \;\; \text{or} \;\; w = -v\,\tan\phi \tag{7.76}$$

where u, v, w, θ_x, θ_y, and θ_z refer to displacements and rotations expressed using the global coordinate system. The material properties are input using a user-defined cylindrical coordinate system. A total of 200 elements and 231 nodes are used in the spatial discretization. Once again, the full tangent preconditioner with the FETI linear solver is used in conjunction with the conjugate gradient method in ADAGIO. Although using the nodal preconditioner will work for this example, better iterative convergence behavior results from using the full tangent preconditioner.

Table 7.3: Analytic and numerical results for transverse deflection at center of cross-ply cylindrical panel under uniform pressure.

Analytic I (in)*	Analytic II (in)+	ADAGIO (in)
0.000695030	0.000694982	0.00070012

*using $m = 1, 3, \ldots, 13$ and $n = 1, 3, \ldots, 13$

+using $m = 1, 3, \ldots, 19$ and $n = 1, 3, \ldots, 19$

Values for the midpoint transverse deflection computed analytically and using ADAGIO are shown in Table 7.3. Once again, using 100 terms in the Fourier series expansion of the analytical solution is deemed to be sufficient, as the midpoint deflection value decreases by only 0.0069% in going from 16 to 100 terms.

Transverse deflection profiles along the $\xi_1 = l_1/2$ and $\xi_2 = l_2/2$ centerlines are shown in Figs. 7.4 and 7.5, respectively. The analytical solutions shown correspond to using 100 terms in the Fourier expansion ($m = 1, 3, \ldots, 19$ and $n = 1, 3, \ldots, 19$). Reasonable agreement has been achieved for the chosen mesh size.

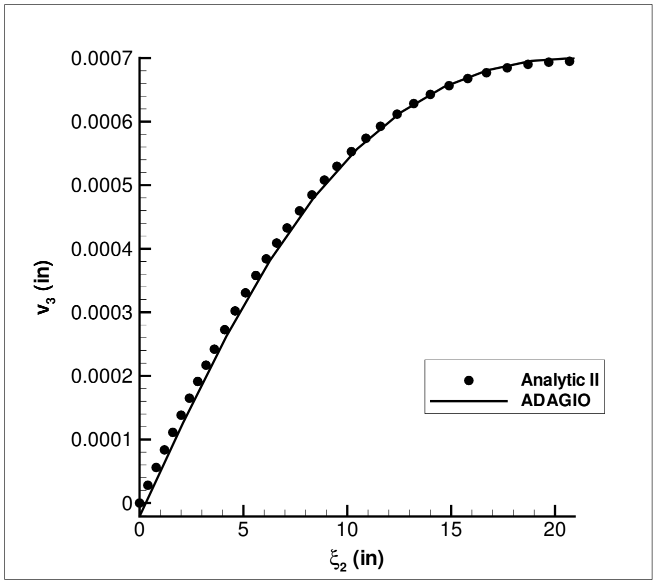

Figure 7.4: Transverse deflection of cross-ply panel along the $\xi_1 = l_1/2$ centerline.

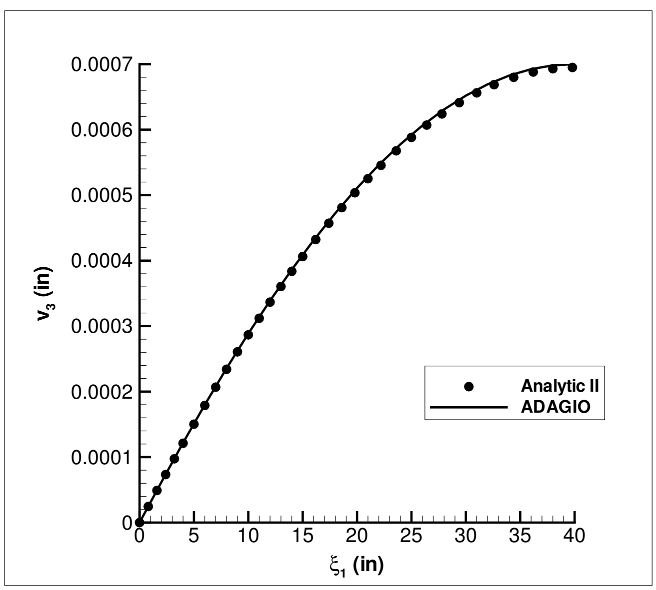

Figure 7.5: Transverse deflection of cross-ply panel along the $\xi_2 = l_2/2$ centerline.

8 Summary

A linear elastic composite shell model has been implemented in ADAGIO and PRESTO. Previously, Sandia has not had a composites capability in its quasi-static and explicit dynamics analysis codes. This new capability will be used in the near future by several customers. Moreover, this model and the orthotropic nonlinear viscoelastic model being implemented by the present author will allow Sandia to pursue partnerships with external customers on various composite topics.

The `elastic_laminate` model can handle any chosen lay-up sequence including the effects of anisotropic thermal expansion. The laminate matrices and thermal force and force-couple resultants are input relative to a user-defined coordinate system which has a lot of flexibility in terms of its construction. Because this model does not require stacking sequence information to be input, the exact layer-wise distribution of stresses cannot be computed. However, an equivalent stress distribution is calculated and available for output for post-processing purposes. The model implementation has been verified using numerous regression tests with analytical solutions. Several of these tests have been presented in this report.

References

[1] Hammerand, D.C., *Critical Time Step for a Bilinear Laminated Composite Mindlin Shell Element*, *Sandia Report* SAND04-XXXX, in preparation, Albuquerque, NM, 2003.

[2] Bathe, K.J., *Finite Element Procedures*, Prentice-Hall, Englewood Cliffs, NJ, 1996.

[3] Flanagan, D.P. and Belytschko, T., "Eigenvalues and Stable Time Steps for the Uniform Strain Hexahedron and Quadrilateral," *Journal of Applied Mechanics*, Vol. 51, 1984, pp. 35–40.

[4] Belytschko, T. and Lin, J.I., "Eigenvalues and Stable Time Steps for the Bilinear Mindlin Plate Element," *International Journal for Numerical Methods in Engineering*, Vol. 21, 1985, pp. 1729–1745.

[5] Hughes, T.J.R., Cohen, M. and Haroun, M., "Reduced and Selective Integration Techniques in Finite Element Analysis of Plates," *Nuclear Engineering Design checkit*, Vol. 46, 1978, pp. 203–222.

[6] Leissa, A.W. and Qatu, M.S., "Equations of Elastic Deformation of Laminated Composite Shallow Shells," *Journal of Applied Mechanics*, Vol. 58, 1991, pp. 181–188.

Appendix A. Input for Fully Constrained Laminate Under Thermal Loading

```
begin sierra elastic_lam_thermal_strain2

  begin definition for function unit
    type is piecewise linear
    ordinate is unit
    abscissa is time
    begin values
      0.0    0.0
      1.0    1.0
    end values
  end definition for function unit

  begin definition for function zero
     type is constant
     begin values
      0.0
     end values
  end definition for function zero

  begin definition for function TEMPERATURE
    type is piecewise linear
    ordinate is temperature
    abscissa is time
    begin values
      0.0   82.0
      1.0  182.0
    end values
  end definition for function TEMPERATURE

  begin definition for function n11
    type is piecewise linear
    abscissa is temperature
    ordinate is nth11
    begin values
      72.0    0.0
     182.0  153.034
    end values
  end definition for function n11


  begin definition for function n22
    type is piecewise linear
    abscissa is temperature
    ordinate is nth22
    begin values
      72.0    0.0
     182.0  146.353
    end values
  end definition for function n22

  begin definition for function n12
    type is piecewise linear
    abscissa is temperature
    ordinate is nth12
```

```
  begin values
    72.0    0.0
   182.0   -1.4543
  end values
end definition for function n12

begin definition for function m11
  type is piecewise linear
  abscissa is temperature
  ordinate is mth11
  begin values
    72.0    0.0
   182.0   -0.0243124
  end values
end definition for function m11

begin definition for function m22
  type is piecewise linear
  abscissa is temperature
  ordinate is mth22
  begin values
    72.0    0.0
   182.0    0.0243124
  end values
end definition for function m22

begin definition for function m12
  type is piecewise linear
  abscissa is temperature
  ordinate is mth12
  begin values
    72.0    0.0
   182.0   -0.0404501
  end values
end definition for function m12


define direction x with vector 1.0 0.0 0.0
define direction y with vector 0.0 1.0 0.0
define direction z with vector 0.0 0.0 1.0

define point pt0 with coordinates 0.0 0.0 0.0
define point ptZ with coordinates 0.0 0.0 1.0
define point ptXZ with coordinates 1.0 0.0 0.0

define coordinate system lam_coord rectangular with point pt0 point ptZ point ptXZ

begin property specification for material linear_elastic
  density         = 1.0

  begin parameters for model elastic_laminate
    youngs modulus = 7.8e6
    poissons ratio = 0.25
    a11 = 243.513e3
    a12 = 51.9604e3
    a16 = -9.82541e3
    a22 = 130.524e3
    a26 = -14.7717e3
    a66 = 75.4072e3
```

```
    a44 = 50.e3
    a45 = 0.0
    a55 = 50.e3
    b11 = -576.117
    b12 = 164.913
    b16 = -419.274
    b22 = 246.291
    b26 = -264.871
    b66 = 164.913
    d11 = 32.3781
    d12 = 6.59888
    d16 = -2.15462
    d22 = 18.1518
    d26 = -3.05374
    d66 = 9.72512
    coordinate system = lam_coord
    direction for rotation = 3
    alpha = 10.0
    theta = 5.0
    nth11 function = n11
    nth22 function = n22
    nth12 function = n12
    mth11 function = m11
    mth22 function = m22
    mth12 function = m12
  end parameters for model elastic_laminate


end property specification for material linear_elastic

begin finite element model mesh1
  Database Name = elastic_lam_thermal_strain2.g
  Database Type = exodusII

  begin parameters for block block_1
    material linear_elastic
    solid mechanics use model elastic_laminate
    shell integration points = 5
    shell integration scheme = trapezoid
    shell scale thickness = 0.04
   #  element strain formulation = strongly-objective
  end parameters for block block_1

end finite element model mesh1

begin adagio procedure Agio_Procedure

  begin time control
      begin time stepping block p1
        start time =  0.0

        begin parameters for adagio region adagio
          time increment = 0.1
        end parameters for adagio region adagio

      end time stepping block p1

      termination time = 1.0
  end time control
```

```
begin adagio region adagio
  use finite element model mesh1
  options = thermalstrain

  prescribed nodal temperature using function TEMPERATURE

  ### output description ###
  begin Results Output output_adagio
    Database Name = elastic_lam_thermal_strain2.e
    Database Type = exodusII
    At Step 0, Increment = 1
    nodal Variables = displacement as displ
    element Variables = bottom_stress as stress_bot
    element Variables = memb_stress as stress_memb
    element Variables = top_stress as stress_top
    element Variables = element_thickness as thick
    element Variables = element_area as area
    element Variables = axis1_dir as axis1
    element Variables = axis2_dir as axis2
    element Variables = ar as ar
    element Variables = as as as
    global Variables = timestep as timestep
  end results output output_adagio

  ### definition of BCs ###

  # bottom left node
  begin fixed displacement
    node set = nodelist_1
    components = x y z
  end fixed displacement

  begin fixed rotation
    node set = nodelist_1
    components = x y z
  end fixed rotation

  # bottom right node
  begin fixed displacement
    node set = nodelist_2
    components = x y z
  end fixed displacement

  begin fixed rotation
    node set = nodelist_2
    components = x y z
  end fixed rotation

  # top right node
  begin fixed displacement
    node set = nodelist_3
    components = x y z
  end fixed displacement

  begin fixed rotation
    node set = nodelist_3
    components = x y z
  end fixed rotation
```

```
    # top left node
    begin fixed displacement
      node set = nodelist_4
      components = x y z
    end fixed displacement

    begin fixed rotation
      node set = nodelist_4
      components = x y z
    end fixed rotation


### ------------------###
### Solver definition ###
### ------------------###

    Loadstep predictor using line search type secant

    Begin adagio solver cg
      Target Residual Tolerance = 1.0e-12
      Maximum Iterations = 5000
      Minimum Iterations = 0
      Orthogonality measure for reset = 0.1
      Line Search type secant
#      preconditioning type nodal translational rotational
      nodal preconditioning type = probe
    end   adagio solver cg

  end adagio region adagio
  end adagio procedure Agio_Procedure

end sierra elastic_lam_thermal_strain2
```

Appendix B. Input for Antisymmetric Angle-Ply Plate Under Uniform Pressure

```
begin sierra laminate_plate_pressure2

  begin definition for function zero
    type is constant
    begin values
      0.0
    end values
  end definition for function zero

  begin definition for function pressure
    type is piecewise linear
    begin values
      0.0       0.0
      1.0      -1.0
    end values
  end definition for function pressure

  define direction x with vector 1.0 0.0 0.0
  define direction y with vector 0.0 1.0 0.0
  define direction z with vector 0.0 0.0 1.0

  define point pt0 with coordinates 0.0 0.0 0.0
  define point ptZ with coordinates 0.0 0.0 1.0
  define point ptXZ with coordinates 1.0 0.0 0.0

  define coordinate system lam_coord rectangular with point pt0 point ptZ point ptXZ

  begin property specification for material shell_material
    density = 1

    begin parameters for model elastic_laminate
      youngs modulus = 26.25e6
      poissons ratio = 0.28
      a11 = 1.26889e6
      a12 = 0.376513e6
      a16 = 0.0
      a22 = 0.274158e6
      a26 = 0.0
      a66 = 0.426188e6
      a44 = 0.426188e6
      a45 = 0.0
      a55 = 0.426188e6
      b11 = 0.0
      b12 = 0.0
      b16 = 3143.99
      b22 = 0.0
      b26 = 1163.74
      b66 = 0.0
      d11 = 676.792
      d12 = 200.807
      d16 = 0.0
      d22 = 146.218
      d26 = 0.0
      d66 = 227.3
```

```
    coordinate system = lam_coord
    direction for rotation = 3
    alpha = 0.0
    theta = 0.0
    nth11 function = zero
    nth22 function = zero
    nth12 function = zero
    mth11 function = zero
    mth22 function = zero
    mth12 function = zero
  end parameters for model elastic_laminate

end property specification for material shell_material

begin finite element model shell_model
  Database Name = laminate_plate_pressure2.g
  Database Type = exodusII

  begin parameters for block block_1
    material shell_material
    solid mechanics use model elastic_laminate
    shell scale thickness = 0.08
  end parameters for block block_1

end finite element model shell_model

begin feti equation solver feti
  local solver = sparse
end

begin adagio procedure shell_procedure

  begin time control
    begin time stepping block p1
      start time = 0.0
      begin parameters for adagio region shell_region
        number of time steps = 1
      end parameters for adagio region shell_region
    end time stepping block p1

    termination time = 1.0

  end time control


  begin adagio region shell_region
    use finite element model shell_model

    begin results output shell_output
      Database Name = laminate_plate_pressure2.e
      Database Type = exodusII
      At Step 0, Increment = 1
      nodal Variables = displacement as displ
      element Variables = element_thickness as thick
    end results output shell_output

    # bottom curve
    begin fixed displacement
      node set = nodelist_10
```

```
        components = y z
      end fixed displacement

      # right curve
      begin fixed displacement
        node set = nodelist_20
        components = x
      end fixed displacement

      begin fixed rotation
        node set = nodelist_20
        components = y z
      end fixed rotation

      # top curve
      begin fixed displacement
        node set = nodelist_30
        components = y
      end fixed displacement

      begin fixed rotation
        node set = nodelist_30
        components = x z
      end fixed rotation

      # left curve
      begin fixed displacement
        node set = nodelist_40
        components = x z
      end fixed displacement

      # applied load
      begin pressure
        surface = surface_100
        function = pressure
        scale factor = 0.003
      end pressure

      Loadstep predictor using line search type secant

      begin adagio solver cg
        Target Residual Tolerance = 1.e-4
        Maximum Iterations = 200
        Minimum Iterations = 5
        Orthogonality measure for reset = 0.1
        Line Search type secant
        Begin full tangent preconditioner
          linear solver = feti
          shell drilling stiffness = 1.0
        End full tangent preconditioner

      end adagio solver cg

    end adagio region shell_region

  end adagio procedure shell_procedure

end sierra laminate_plate_pressure2
```

Appendix C. Input for Cross-Ply Cylindrical Panel Under Uniform Pressure

```
begin sierra laminate_cyl_panel_press

  begin definition for function zero
    type is constant
    begin values
      0.0
    end values
  end definition for function zero

  begin definition for function pressure
    type is piecewise linear
    begin values
      0.0       0.0
      1.0      -0.003
    end values
  end definition for function pressure

  define direction x with vector 1.0 0.0 0.0
  define direction y with vector 0.0 1.0 0.0
  define direction z with vector 0.0 0.0 1.0

  define direction dirA with vector 0.0 0.207912 0.978148

  define point pt0 with coordinates 0.0 20.7912 -98.8148
  define point ptZ with coordinates 1.0 20.7912 -98.8148
  define point ptXZ with coordinates 0.0 20.7912 1.0

  define coordinate system lam_coord cylindrical with point pt0 point ptZ point ptXZ

  begin property specification for material shell_material
    density = 1

    begin parameters for model elastic
      youngs modulus = 18.e6
      poissons ratio = 0.34
    end parameters for model elastic

    begin parameters for model elastic_laminate
      youngs modulus = 18.e6
      poissons ratio = 0.34
      a11 = 3.13216e6
      a12 = 153702.
      a16 = 0.0
      a22 = 3.13216e6
      a26 = 0.0
      a66 = 288000.0
      a44 = 3.2e6
      a45 = 0.0
      a55 = 3.2e6
      b11 = 0.0
      b12 = 0.0
      b16 = 0.0
      b22 = 0.0
      b26 = 0.0
      b66 = 0.0
```

```
    d11 = 43880.4
    d12 = 1311.59
    d16 = 0.0
    d22 = 9575.16
    d26 = 0.0
    d66 = 2457.6
    coordinate system = lam_coord
    direction for rotation = 3
    alpha = 0.0
    theta = 90.0
    nth11 function = zero
    nth22 function = zero
    nth12 function = zero
    mth11 function = zero
    mth22 function = zero
    mth12 function = zero
  end parameters for model elastic_laminate

end property specification for material shell_material

begin finite element model shell_model
  Database Name = laminate_cyl_panel_press.g
  Database Type = exodusII

  begin parameters for block block_1
    material shell_material
    solid mechanics use model elastic_laminate
    shell integration points = 5
    shell integration scheme = trapezoid
    shell scale thickness = 0.32
  end parameters for block block_1

end finite element model shell_model

begin feti equation solver feti
  local solver = sparse
end

begin adagio procedure shell_procedure

  begin time control
    begin time stepping block p1
      start time = 0.0
      begin parameters for adagio region shell_region
        number of time steps = 1
      end parameters for adagio region shell_region
    end time stepping block p1

    termination time = 1.0

  end time control


  begin adagio region shell_region
    use finite element model shell_model

    begin results output shell_output
      Database Name = laminate_cyl_panel_press.e
      Database Type = exodusII
```

```
      At Step 0, Increment = 1
      nodal Variables = displacement as displ
      element Variables = element_thickness as thick
#       element variables = axis1_dir as axis1
#       element variables = axis2_dir as axis2
    end results output shell_output

    # right curve
    begin fixed displacement
      node set = nodelist_20
      components = y z
    end fixed displacement

    # top curve
    begin prescribed displacement
      node set = nodelist_30
      direction = dirA
      function = zero
      scale factor = 1.0
    end prescribed displacement

    begin fixed displacement
      node set = nodelist_30
      components = x
    end fixed displacement

    # left curve
    begin fixed displacement
      node set = nodelist_40
      components = x
    end fixed displacement

    begin fixed rotation
      node set = nodelist_40
      components = y z
    end fixed rotation

    # bottom curve
    begin fixed displacement
      node set = nodelist_10
      components = y
    end fixed displacement

    begin fixed rotation
      node set = nodelist_10
      components = x z
    end fixed rotation

    # applied load
    begin pressure
      surface = surface_100
      function = pressure
    end pressure

    Loadstep predictor using line search type secant

    begin adagio solver cg
      Target Residual Tolerance = 1.e-4
      Maximum Iterations = 200
```

```
        Minimum Iterations = 5
        Orthogonality measure for reset = 0.1
        Line Search type secant
        Begin full tangent preconditioner
          linear solver = feti
          shell drilling stiffness = 1.0
        End full tangent preconditioner
      end adagio solver cg

    end adagio region shell_region

  end adagio procedure shell_procedure

end sierra laminate_cyl_panel_press
```

Distribution

1	MS 0372	J. Jung, 9127
1	MS 0372	R. May, 9126
1	MS 0380	K. Alvin, 9142
1	MS 0380	M. Blanford, 9142
1	MS 0380	J. Hales, 9142
1	MS 0380	M. Heinstein, 9142
1	MS 0380	A. Gullerud, 9142
1	MS 0380	S. Key, 9142
1	MS 0380	R. Koteras, 9142
1	MS 0380	J. Mitchell, 9142
1	MS 0380	K. Pierson, 9142
1	MS 0380	V. Porter, 9142
1	MS 0380	G. Reese, 9142
1	MS 0555	M. Garrett, 9122
1	MS 0557	T. Baca, 9125
1	MS 0615	D. Roach, 6252
1	MS 0847	H. Morgan, 9120
1	MS 0847	J. Redmond, 9124
1	MS 0847	H. Walther, 9127
1	MS 0888	D. Adolf, 1811
1	MS 0893	File Copy
1	MS 0893	R. Chambers, 9123
1	MS 0893	J. Cox, 9123
1	MS 0893	C. Lo, 9123
15	MS 0893	D. Hammerand, 9123
1	MS 0893	C. Lavin, 9123
1	MS 0893	M. Neilsen, 9123
1	MS 0893	J. Pott, 9123
1	MS 0893	E. Reedy, 9123
1	MS 0893	W. Scherzinger, 9123